The Pennsylvania State University

The Graduate School

Electrical Engineering

UNSUPERVISED IDENTIFICATION OF TISSUES IN ZEBRAFISH

A Thesis in

Electrical Engineering

by

Harshil Shah

Submitted in Partial Fulfillment
of the Requirements
for the Degree of

Master of Science

May 2016

The thesis of Harshil Shah was reviewed and approved* by the following:

David Miller
Professor of Electrical Engineering
Thesis Advisor

John Doherty
Professor of Electrical Engineering

Kultegin Aydin
Professor of Electrical Engineering
Head of the Department of Electrical Engineering

*Signatures are on file in the Graduate School

ABSTRACT

This project is a part of the medical imaging research going on at Hershey Medical Center. Given an image of a zebrafish, the task is to classify the different tissues such as the notochord and spinal cord tissues of the zebrafish. Images of the zebrafish were obtained from Dr. Cheng at Hershey Medical Center. This is basically an image segmentation problem. We take an unsupervised approach to classify the tissues in the image. Active-contour models are used along with narrowband level sets to identify and segment out the notochord tissue from the image. The objective function of the contour is obtained from the active-contour models, which is minimized using level sets. Active-contour models also help in detecting the internal contours automatically. The aim is to experiment with different hyper parameters like the size of the mask, smoothening parameter and the number of iterations to achieve the best accuracy for tissue identification and segmentation. Accuracy of the proposed approach will be evaluated using True Positive Rate and the ratio of False Positive Count to the True Positive Count. This work will help speed up the ongoing genomics research at Hershey Medical Center.

TABLE OF CONTENTS

LIST OF FIGURES

LIST OF TABLES

ACKNOWLEDGEMENTS

First and foremost I would like to thank my advisor, Dr. David Miller. Dr. Miller has always been very supportive throughout my research, he has always been there providing guidance and answering all my queries without any hesitation. His expertise in machine learning is amazing and I am thankful to him that he gave me a chance to work under him. He has motivated me and always kept me on my toes through the year. I would also like to thank Dr. John Doherty. He was my temporary advisor when I first came to Penn State, and he gave me lots of support. He gave me my first part time job as a grader and since then I have just seen upwards. Another special thanks goes to my family who have supported me through all my endeavors without any reservations. My roommates Priyan Gada, Meet Shah, Amal Agarwal, Neel Shah and Manav Desai, all have been very supportive and always had my back. Nachiket Kare another colleague has been very helpful through my research. Last but not the least I would like to thank Pennsylvania State University for this wonderful opportunity to study at the prestigious Electrical Engineering Department.

Chapter 1

Introduction

The area of biomedical image processing has always been an interesting field. This field has been demanding lots of research in the past few years. The best part about research in this field, is the opportunity to work on real life problems and chance to make a difference in the world. Medical imaging is very appealing because the technology that we work on has a direct impact on our lives. For example through this research, lots of mysteries about the zebrafish that otherwise have been causing trouble in the past can be solved. This topic in spite of being very challenging is extremely interesting and of great importance for the research going on at Hershey. Zebrafish is one of the few species which are of great research importance. Other important species include rats, rodents, rabbits etc.

Zebrafish is also known as Danio rerio. The use of zebrafish as a model organism has started in the 1960s. It is a tropical fish which in its larval stages is transparent. This helps is studying the blood vessels and functioning of vital organs during the developmental stages. They have already been used to study the biological process behind muscular dystrophy and also are very important to study diseases like cancer. Zebrafish is widely used for research since it's small, easy to store and also reproduce at an extremely fast rate. In addition to this they share 70 percent of the genes with humans and have a similar genetic structure. Only rats have more similarity to humans. All these reasons make zebrafish one of the ideal research organisms. In today's time more than 500 research laboratories across the world study zebrafish as a premier vertebrate model system, and Hershey Medical center is one of them.

Dr. Cheng and his research team at Hershey Medical Center want us to develop an image segmentation tool which will differentiate different tissues inside the zebrafish. The image data given to us consists of 1350 2-D image slices. Dr. Cheng's students have also given us ground truth labelled images which mark the tissues inside the image. This data is useful in establishing the ground truth so that our algorithm output can be verified and its efficiency can be measured accurately.

I have taken up this project so that I can experiment with different feature extraction, image processing techniques and also get to work on different image segmentation techniques. Implementing all these techniques on a set of almost 1300 images and extracting important information from them is something which sounds very interesting. Also, these techniques can also be implemented on different types of image data such as geological imaging data, social media data such as Instagram and in image processing specific tasks such as face detection and object identification. The feature extraction techniques should be common to different types of images. Below are a couple of sample images of zebrafish that have been obtained as part of the data set from the researchers at Hershey.

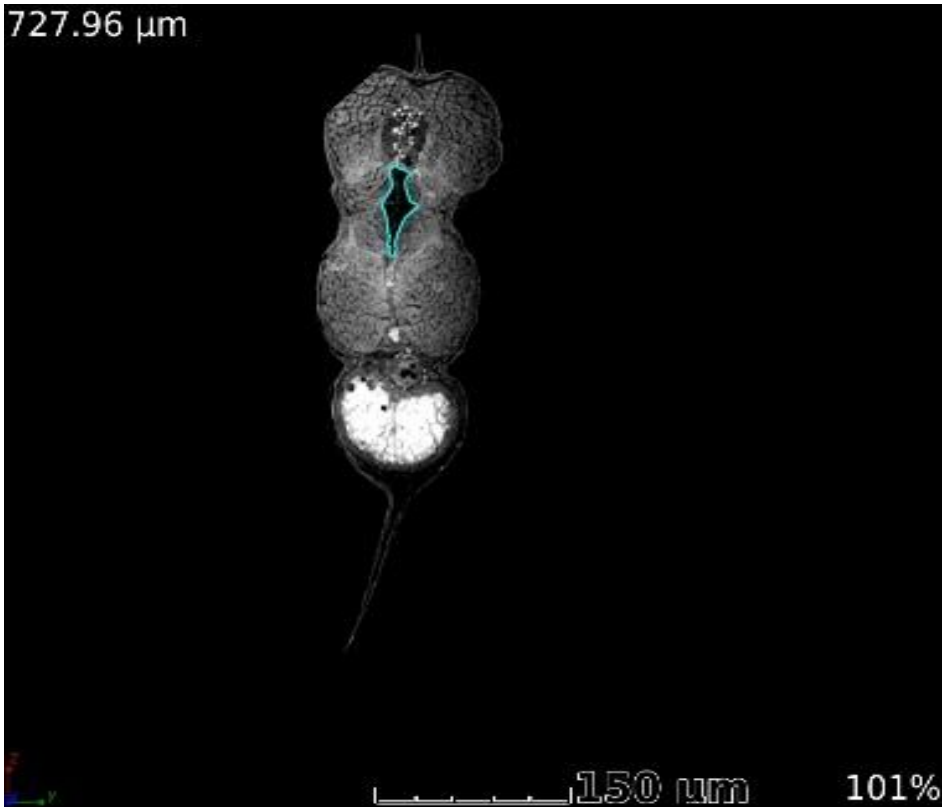

Figure 1-1. Sample ground truth image in which the notochord tissue is denoted as the region inside the blue border.

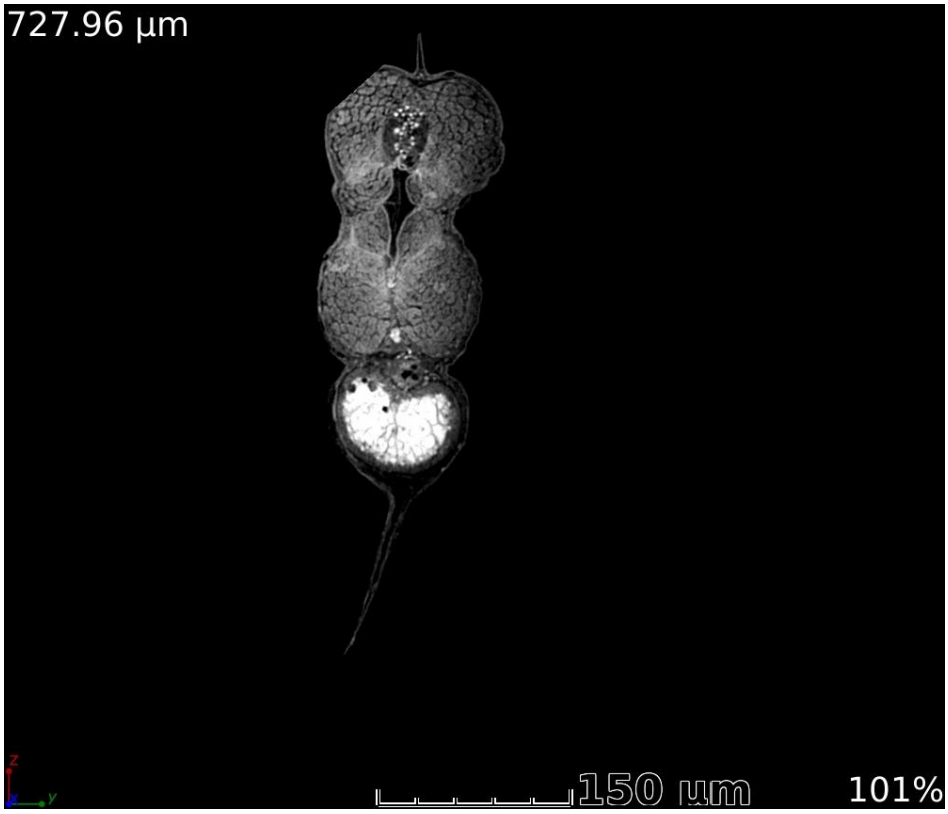

Figure 1-2. Sample image in which the notochord tissue needs to be segmented.

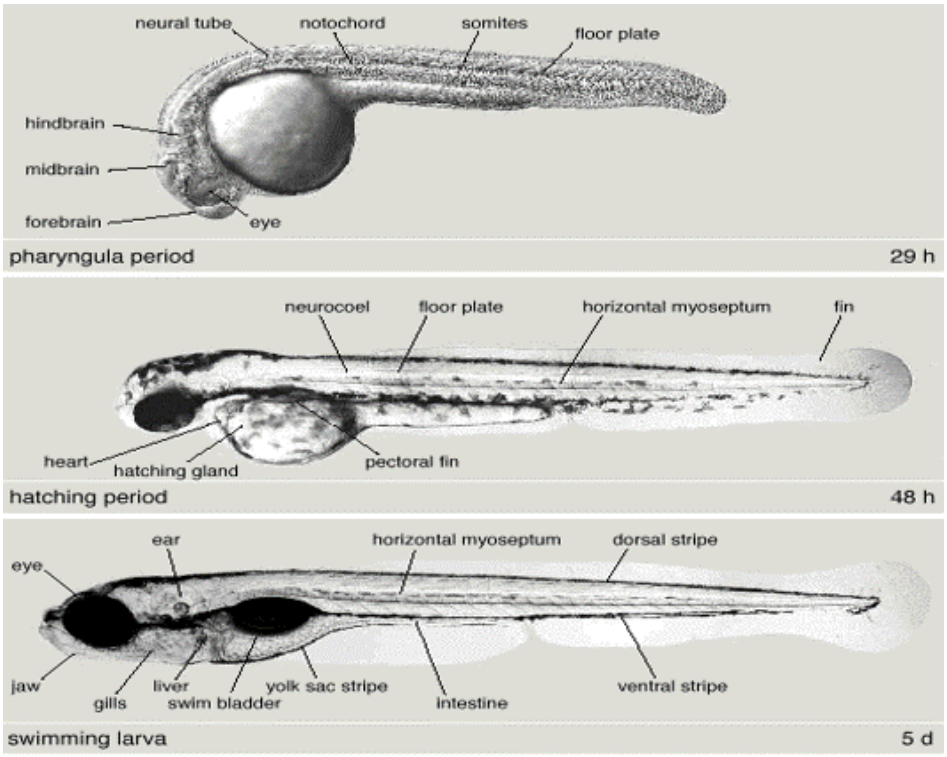

Figure 1-3. Image of Zebrafish with notochord tissue shown.

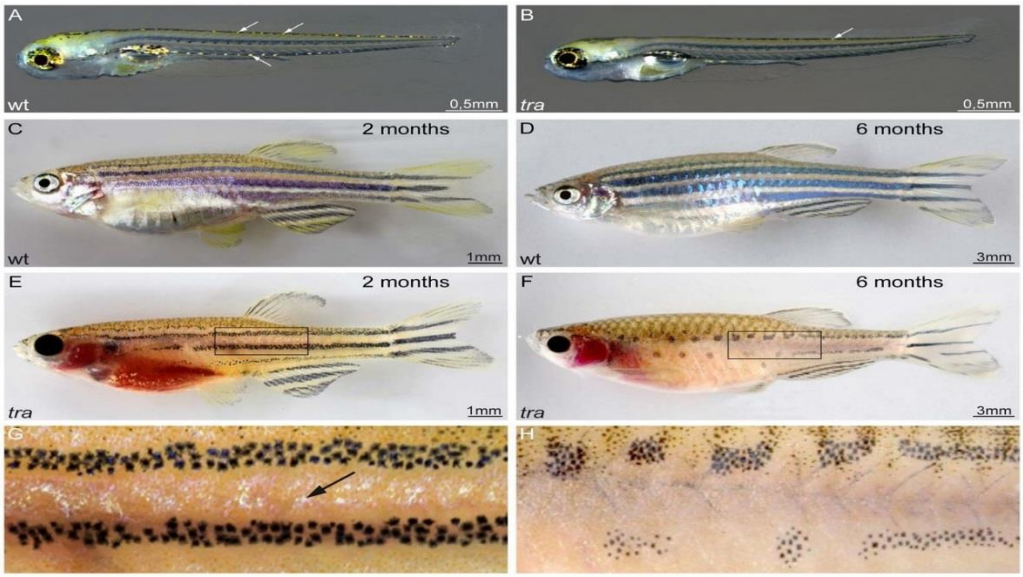

Figure 1-4. Transparency of Zebrafish during the larval stages.

Contribution

In all this genomic research, a lot of time is spent by scientists, students in analyzing the changes which occur when a protein is injected. To speed up this process of analyzing the changes, the zebrafish is sent to a Micro-CT imaging center. The image which is obtained from that imaging center is a 3 dimensional image of the zebrafish. The raw image files obtained from the imaging center are around 114 gigabytes. These files are processed by Dr. Cheng's PhD students. The resulting 3-D image is made up of 1350 2-D images. The task at hand is to develop a system for automatically segmenting different tissues inside the zebrafish. If this is accomplished, it will significantly speed up the time required for analyzing the zebrafish images and draw some conclusions. My aim is to propose an efficient image segmentation technique and to streamline the process of segmentation, so that this method can be used further in the research. I have taken over from where my senior Niranjan Yardi has left off. Niranjan had worked on this project a year ago and proposed an approach which did not solve the problem at hand entirely. I have undertaken a completely different approach which will be explained in detail further ahead. One of the major differences between his approach and the one that I have proposed is that, his approach was supervised whereas the approach in this thesis is unsupervised. I hope to fulfill the requirements of Dr. Cheng at Hershey and provide a suitable method for them to speed up their research.

Outline

The overall outline of this work is as follows: Chapter 2 reviews previous work related to our study. Chapter 3 explains the active-contour method. Chapter 4 explains the level set method. Chapter 5 explains the algorithm that I have used in this thesis. Chapter 6 explains the data set. Chapter 7 contains the experimental observations and results. Chapter 8 has the conclusion and future work. All this is then followed by references and Appendix-A, Appendix-B which have individual error rates for the images.

Chapter 2

Literature Review

This is basically an image segmentation problem wherein we have to segment the zebrafish tissue into different regions. Image segmentation is a hot topic of research and has been widely studied. We divide segmentation methods into eight categories: (a) thresholding approaches, (b) region growing approaches, (c) classifiers, (d) clustering approaches, (e) Markov random-field (MRF) models, (f) artificial neural networks, (g) Active contour models, and (h) atlas-guided approaches. Region growing is a technique for extracting an image region that is connected based on some criteria. The method proceeds by first initializing a pixels or group of pixels as pixels of interest. The region then grows and adds more pixels to this collection based on some defined criteria. This criteria can be based on features in the image. We would like to experiment with active-contour models to segment out the notochord tissue from the rest of the image. In this thesis we are going to try out the active-contour models for segmenting out the notochord tissue, which is also known as snake models. Once we obtain the segment, we will compare each pixel to the ground truth to determine whether a particular pixel is a notochord tissue or not.

Active contour models also known as snake models are generally used to obtain object boundaries in 2-d images. Active-contours are based on energy minimization guided by external constraint forces and influenced by image forces that it pull towards features such as lines and edges, as mentioned in [2]. This method is also used for detection of lines, edges and subjective contours, motion tracking and stereo-matching. Such active-contour models are based on edge-function and image gradient. The discrete gradients are bounded and never zero on the edges. If the image is very noisy, strong smoothing will be required which will eventually smoothen out the edges. Thus [1] has proposed a different active-contour model without a stopping criterion for

edges i.e. it is not based on the image gradient. Instead the stopping criterion is based on upon energy minimization, Mumford-Shah segmentation techniques [5] and level sets. This helps in detecting objects with both smooth as well as discontinuous boundaries. With the help of the algorithm defined in [1], active-contours can be found anywhere within the image. Another important factor to note is that interior contours are detected automatically.

Level sets are widely used for analysis of surfaces and shapes. [9] uses level sets for 3-d reconstruction of range data. [9] uses Maximum A Posteriori [MAP] strategy to combine data with known properties or tendencies of the measurement of surfaces. Finding these surfaces with highest likelihood is a nonlinear optimization problem. In spite of level sets being widely used, there are many disadvantages associated with it like very large computations are required. Also level sets do not represent the surface during deformation i.e., when the contour grows or shrinks very effectively. In order to deal with these short-comings [9] uses sparse-field algorithms to deal with the growing computational complexities. Sparse-field algorithms ensure a set of active points defined for the curve which are visited and updated during each iteration. These set of active points are a set of grid points through which the model passes and helps in the evolution of the curve.

[1] has been used as a reference for the implementation of the active-contour algorithm. This paper uses active-contours along with level sets for the purpose of image segmentation. Level sets help provide complex curve behavior. In order to improve the computation complexity of the level sets, sparse-field algorithm can be used. Active-contours, level sets and sparse-field algorithm together form a very powerful image segmentation algorithm, which can be used on different kinds of images. In the next few chapters we will explain active-contours, level sets in more detail, followed by the automated algorithm proposed to classify the notochord tissue in zebrafish and some results and conclusions to follow that.

Other related works are [3] [11] and [10] that use active contours and image segmentation.

Chapter 3

Active Contour

In this section we will discuss the active-contour algorithm given in [1]. In classical times the snake model or the active-contour model which depends on an edge function as a stopping criterion was widely used. This model was used till the active-contour without edges was introduced. The new algorithm will work on extremely noisy images also and we need not worry about smoothening the image and in the process smoothen out the edges and contours.

Let's consider that an image i is made up of two regions with piecewise constant intensities of distinct values $i^i \; and \; i^0$. The object of interest is present in the inner region i^i . Let the boundary be denoted by C_o. We know define the fitting term or the energy term as follows:

$$F(C) = F_1(C) + F_2(C) = \int_{inside\ C} |i(x,y) - c_1|^2 \, dxdy + \int_{outside\ C} |i(x,y) - c_2|^2 \, dxdy$$

Where $c_1 = Average\ inside\ the\ curve$

$c_2 = Average\ outside\ the\ curve$

$C = any\ point\ on\ the\ curve\ on\ whom\ c_1\ and\ c_2\ depend\ upon.$

Since this algorithm is based on energy minimization, hence we have to minimize the above term. It is seen that we obtain minimization when $C = C_o$ i.e. the curve C is on the boundary of the object.

$$F_1(C) + F_2(C) \approx 0 \approx F_1(C_o) + F_2(C_o)$$

If the curve C is outside the object then,

$F_1(C) > 0 \; and \; F_2(C) \approx 0$

If the curve C is inside the object then,

$F_1(C) \approx 0 \; and \; F_2(C) > 0$

If the curve C is inside the object and outside the object then,

$F_1(C) > 0 \; and \; F_2(C) > 0$

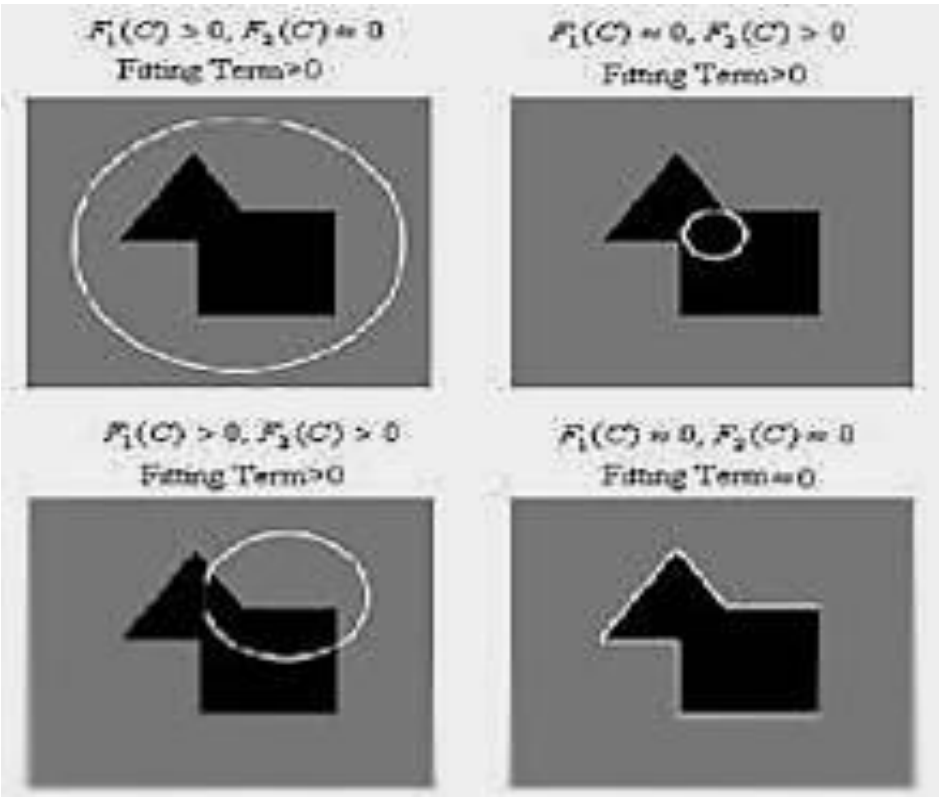

Figure 3-1. Cases for minimization of the energy term in Active-contour.

Regularization terms are also added to the energy term in order to achieve better minimization.

Regularization terms could either be the length of the curve or the area inside the curve. [1] uses

narrowband level sets to achieve minimization. This concept is explained in the following chapter.

Chapter 4

Level Sets

Level set methods is the concept of using level sets for numerical analysis of surfaces. This method makes it easy to follow surfaces that change shape i.e. surface splits into two or it

develops holes etc. In two dimensions level set method represents a closed curve or object boundary Γ using a function ϕ called the level set function. Γ is represented as the zero-level set of ϕ as $\Gamma = \{(x, y)|\phi(x, y) = 0\}$, where ϕ is assumed to take positive values inside the region limited by the curve Γ and negative values outside the curve.

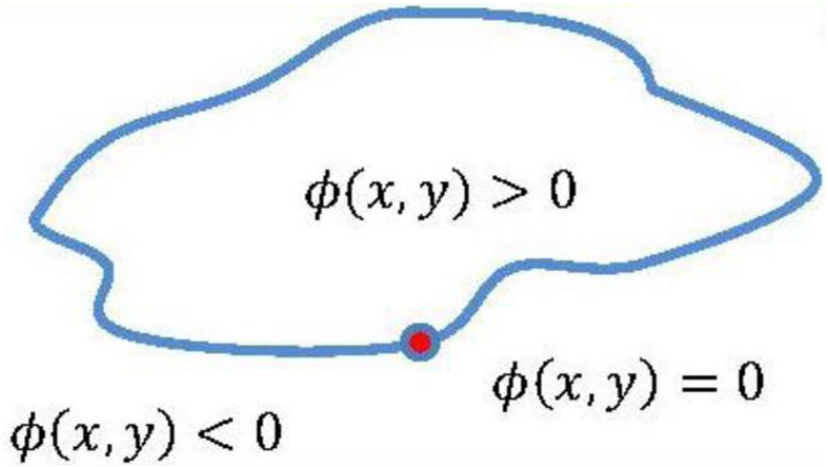

Figure 4-1. Level set representation of the boundary of an object.

The Osher-Sethian level set method described in [7], tracks the motion of the region of interest by embedding the region as the zero level of the signed distance function. The motion is matched to the zero-level set of the level set function, and the resulting initial value partial differential equation of the level set function resembles the Hamilton –Jacobi equation. In this setting, curves and contours are easily evaluated and changes in the shape take place in a natural manner. The advantage of using the level set method is that it is accurate robust and versatile for a wide variety of problems. It can handle sharp corners as well as changes in the shape of the region of interest. The details on how the concept of level set methods was used in the active-contour algorithm to minimize the objective function is shown below.

We know that the initial ϕ can be any arbitrary function as long as it satisfies the condition - $\Gamma = \{(x,y)|\phi(x,y) = 0\}$. Given an initial ϕ at $t = 0$, it would be possible to know ϕ at any time *t* with the motion equation $\frac{d\emptyset}{dt}$. Using the chain rule we get the following,

$$\frac{d\emptyset(x(t),t)}{dt} = 0$$

$$\frac{d\emptyset}{dx(t)}\frac{dx(t)}{dt} + \frac{d\emptyset(t)}{dt} = 0$$

$$\frac{d\emptyset}{dx(t)}x_t + \emptyset_t = 0$$

We know that $\frac{d\emptyset}{dx} = \nabla\emptyset$. Also the speed of x_t *which in our case is* $(x,y)_t$ is given by a force normal to the surface. This force is nothing but the energy term or fitting term defined in the earlier chapter using level sets. Thus we can rewrite the equation of motion as follows:

$$\frac{d\emptyset}{dt} + F.\nabla\emptyset = 0$$

Normal to Γ is given as

$$F_N = F.\frac{\nabla\emptyset}{|\nabla\emptyset|}$$

where,

$$\frac{d\emptyset}{dt} = sgn(\emptyset)(1 - |\nabla\emptyset|)$$

$sgn(\emptyset)$ *is defined as,*

$$sgn(\emptyset) = 2H(x) - 1,$$

$$where, H(x) = 1\ if\ x > 0$$

$$H(x) = 0\ if\ x < 0$$

Thus we get the final equation as:

$$\frac{d\emptyset}{dt} + F_N|\nabla\emptyset| = 0$$

$|\nabla\emptyset|$ is solved using partial differential equations by the finite difference method. This is done to discretize the values. Also the movement of the boundary is bounded by CFL condition. Courant-Friedrichs-Lewy (CFL) condition is a necessary condition for convergence while solve partial differential equations by the finite difference method. Since the movement of the boundary is bounded by the above condition, it is possible to restrict the level set process as a band around the zero level set without losing flexibility or distorting the result. Narrow band around the boundary is initially using the signed distance function (SDF).

Signed distance function of a set ω determines the distance of a given point x from the boundary of ω, with the sign given determined by whether x is in ω or not. In our case we take a binary mask and calculate the distance of each pixel from the nearest non-zero pixel. This will give us the narrow band around the boundary of the mask. Euclidean distance between each pixel and its nearest non-zero pixel is calculated. Euclidean distance is the straight line distance between two pixels. This concept will be made clearer with the illustrations below.

Figure 4-2. Example of how Signed Distance Function works.

Table 4-1. Another example of how Signed Distance Function works.

0	**0**	**0**	**0**	**0**	**1.4142**	**1**	**1.4142**	**2.2361**	**3.1623**
0	**1**	**0**	**0**	**0**	**1**	**0**	**1**	**2**	**2.2361**
0	**0**	**0**	**0**	**0**	**1.4142**	**1**	**1.4142**	**1**	**1.4142**
0	**0**	**0**	**1**	**0**	**2.2361**	**2**	**1**	**0**	**1**
0	**0**	**0**	**0**	**0**	**3.1623**	**2.2361**	**1.4142**	**1**	**1.4142**

In our case we take the SDF of the original mask, then the SDF of the complement of the original mask. We then subtract both and add it to the original mask in order to obtain narrowband level set.

$$Narrowband\ Level\ Set$$
$$= SDF(Original\ Mask) - SDF\big(complement(Original\ Mask)\big)$$
$$+ Original\ Mask$$

Table 4-2. Original mask on the left. SDF of the mask on the right.

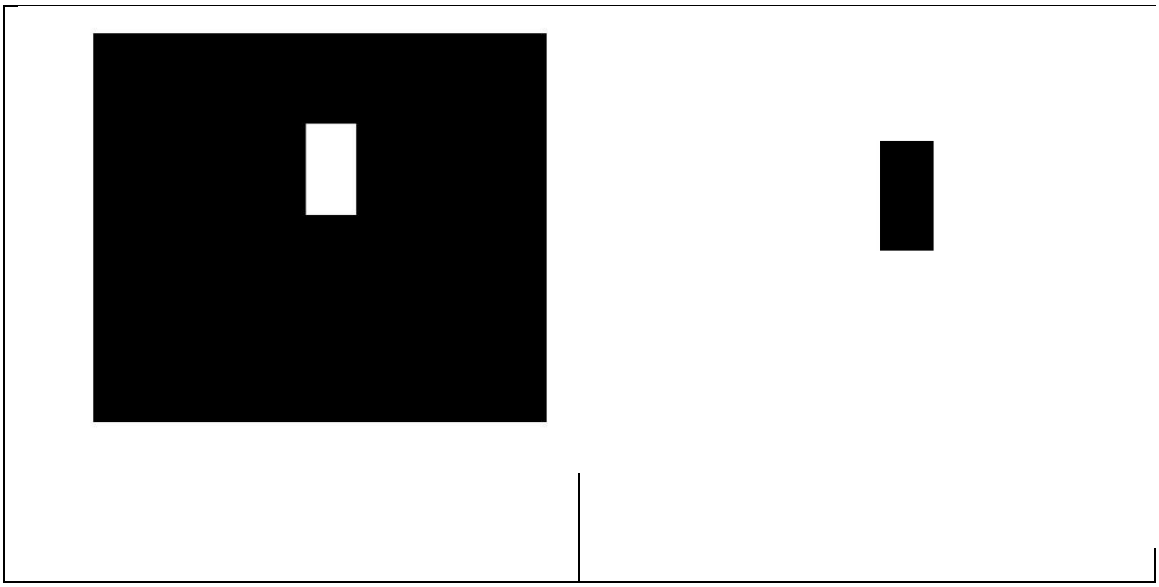

Table 4-3. Complement of the original mask on the left. SDF of the complement on the right.

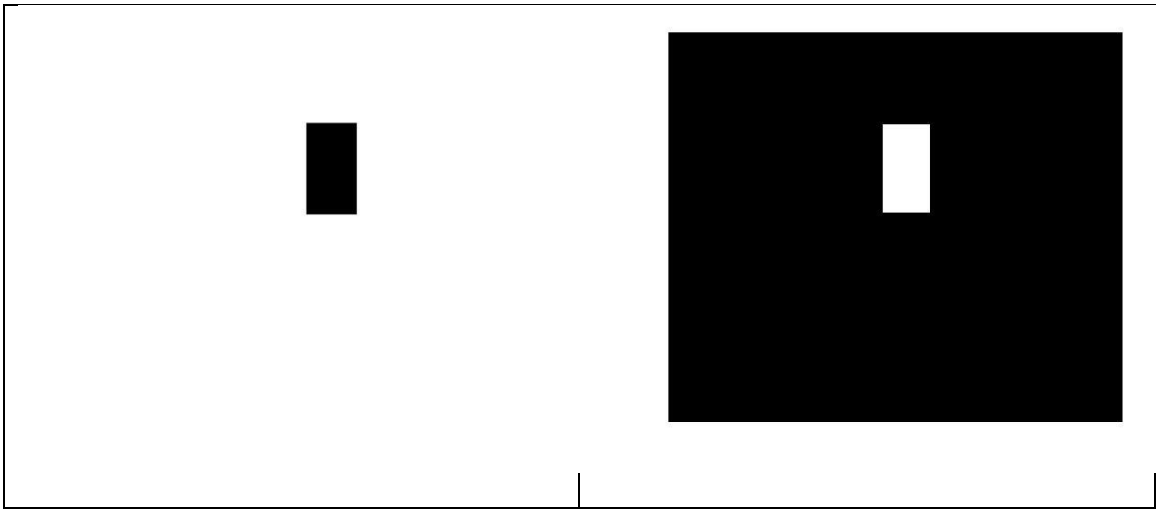

Figure 4-3. Resulting narrowband level set of the initial mask.

The following chapter will explain the details about the automated algorithm proposed to identify notochord tissues.

Chapter 5

Automated Identification and Segmentation of Notochord Tissue

In order to achieve segmentation of the notochord tissue, the algorithm mentioned in [1] was used. This segmentation algorithm was obtained from [13].

Pseudo-code for the segmentation algorithm, is as follows:

1. *Initialize the smoothening factor to a default value if not mentioned in the input Its value generally ranges between 0 – 1. Default value is taken to be 0.2.*
2. *Convert the input image to a grayscale image of type double.*
3. *Create a signed distance map from the mask. Distance of each pixel to the nearest nonzero element. This is used to initialize the narrow band around the curve as shown previously.*
4. *Calculate the Energy of the curve using the narrow band, interior mean and exterior mean.*

$$F(C) = F_1(C) + F_2(C) = \int_{inside\ C} |i(x,y) - c_1|^2\, dxdy + \int_{outside\ C} |i(x,y) - c_2|^2\, dxdy$$

5. *Using the neighboring pixels of the narrow band and central derivatives, minimize the energy.*

$$\frac{d\emptyset}{dt} + F_N|\nabla\emptyset| = 0$$

6. *Evolve the curve, smoothen the curve and display the intermediate output.*
7. *Perform the above steps till the max no of iterations specified in the input.*
8. *The segmented image is obtained at the end of the algorithm.*

Identification of Notochord Tissue using Method - I:

1. *Initialize a binary mask of the same size as the input image. Define a rectangular patch of 1's as follows: mask (200:400,470:580) =1.*
2. *The above mask is chosen after experimentation with other ranges.*
3. *Resize both the input image and the mask for faster computations.*
4. *Input image, mask and the no of iterations all are given as input to the segmentation algorithm.*
5. *Segmented image is given at the output of the algorithm.*
6. *True Positive Rate and ratio of False Positive Count to True Positive Count are calculated to evaluate the accuracy of the segmentation algorithm.*

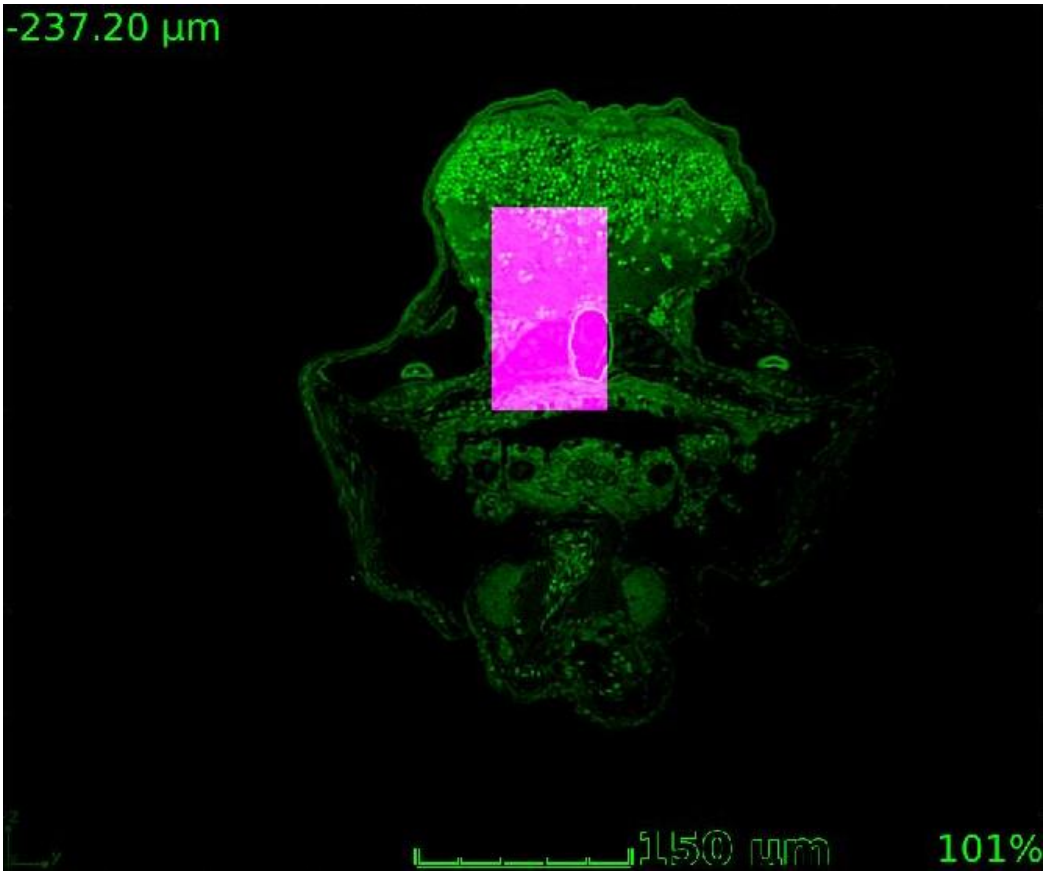

Figure 5-1. Above image shows the rectangular shaped initial mask which is pink in color. The green portion is the test image of the zebrafish.

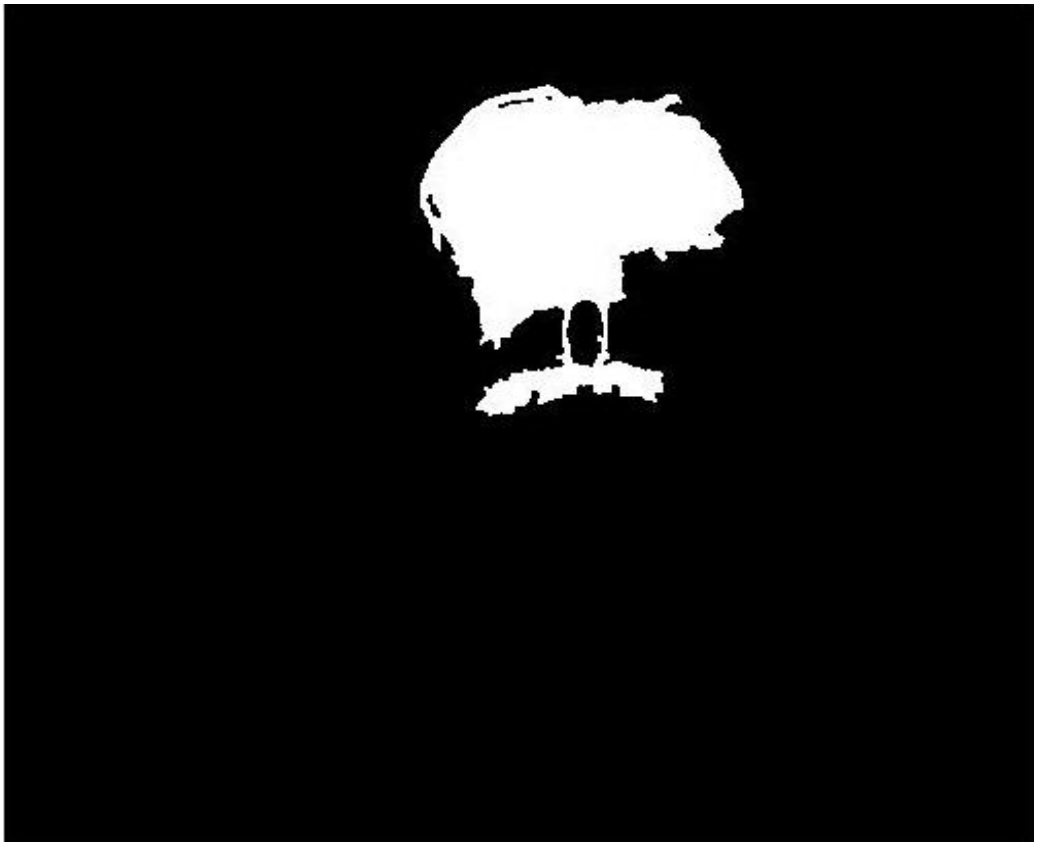

Figure 5-2. Segmented image obtained using the initial mask and input image shown above.

After analysing the accurate functioning of the segmentation algorithm, I propose the following automated algorithm which selects a particular mask for each image based upon the grayscale values of the segmented image. This way we do not need to initialize a mask for each image. Only a set of 5 or even more if required masks should be initialized beforehand, then when the algorithm will run on a data set of large number of images, it will decide an appropriate mask to use for each image and then we can evaluate the selected segmentations using true positive rate and ratio of false positive count to true positive count.

Identification of Notochord Tissue using Method – II:

1. *One time initialization of 5 binary masks of the same size as the input image. Number of masks can be increased as required.*
2. *Resize all the masks and the input image for faster computations.*
3. *Give each mask, input image and no of iterations to the segmentation algorithm.*
4. *5 segmented images, one for each mask are obtained.*
5. *Calculate the mean grayscale for each of the segmented grayscale images.*
6. *Check if any of the 5 values of the mean grayscale is less than 20, if yes then assign the value 250 to it. If the mean grayscale is less than 20 that means the segmented image is incorrect and the region consists only of the background. This is done to check whether the notochord tissue is correctly segmented or we get only background pixels which are black (grayscale value = 0). Hence we check whether the mean grayscale value is less than 20 or not.*
7. *Select the mask with the lowest mean grayscale value > 20.*
8. *Check if all the 5 values of mean grayscale is equivalent to 250, if yes that means the initialized masks are incorrect for that particular image and need to redefine the 5 masks.*
9. *Calculate the true positive rate and ratio of false positive count to true positive count for the selected masks for each image to evaluate its accuracy.*
10. *Another approach instead of step 9 would be to find the mask which is selected to have the least mean grayscale value most number of times for all the images and then evaluate the true positive rate and ratio of false negative count to true positive count using that selected mask on all images.*

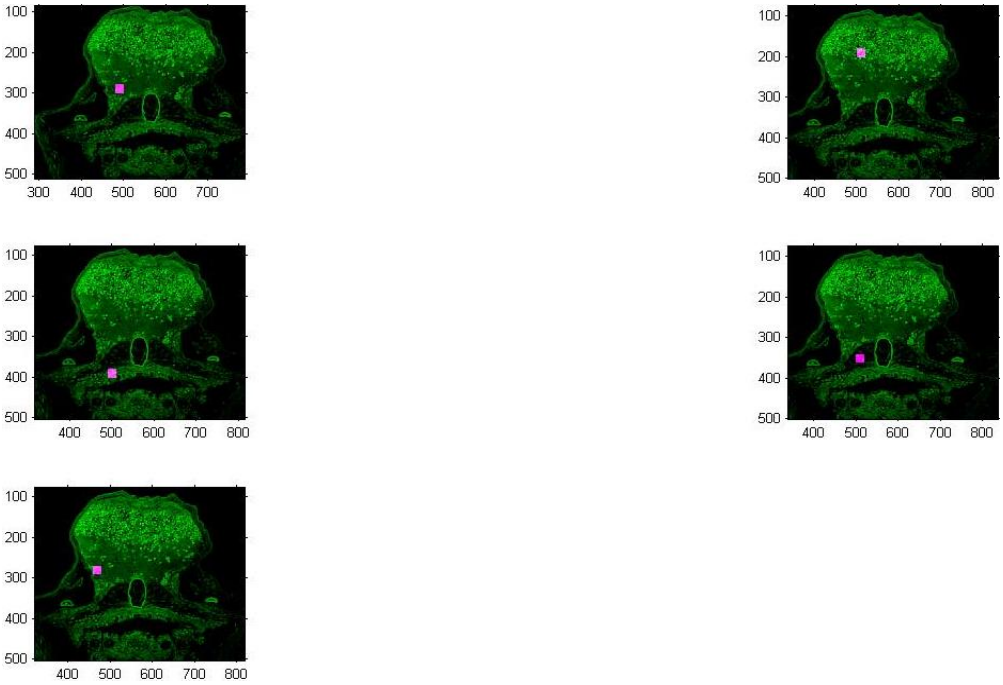

Figure 5-3. Position of all the initial masks w.r.t to the notochord tissue. Pink squares are the initial masks and green portion is the image of the zebrafish.

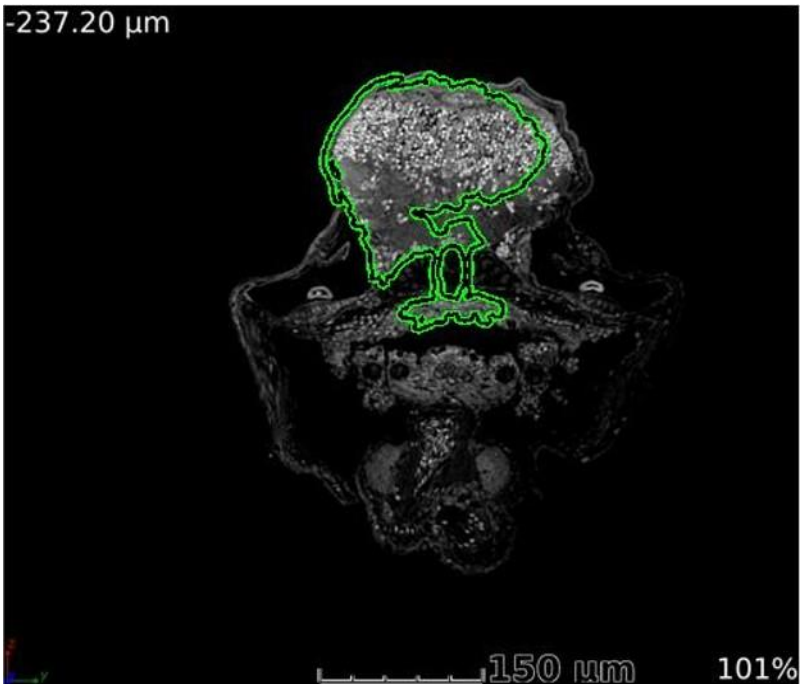

Figure 5-4. Final segmentation using mask 1. Grayscale value = 60.7714

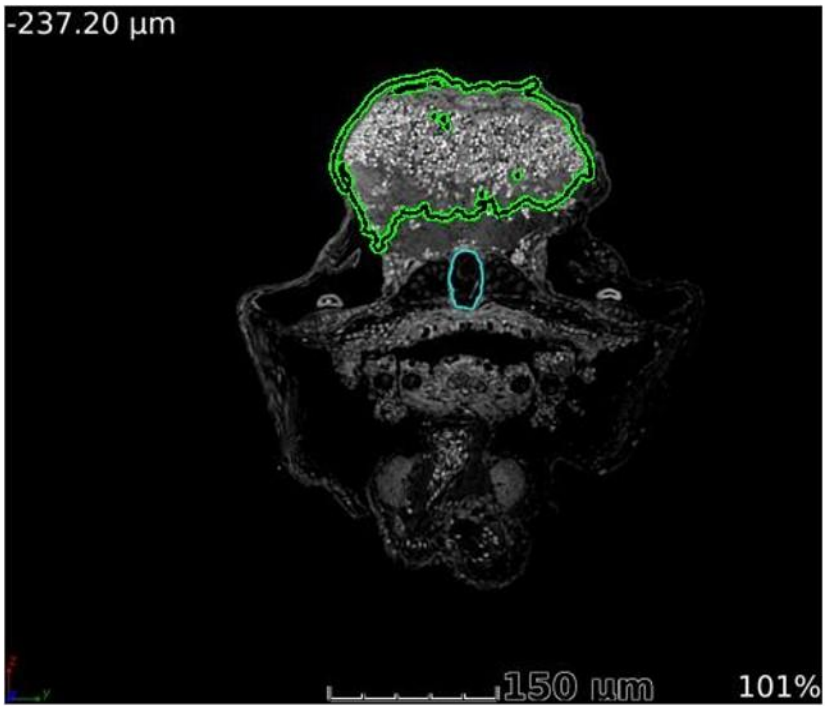

Figure 5-5. Final segmentation using mask 2. Grayscale value = 82.2643

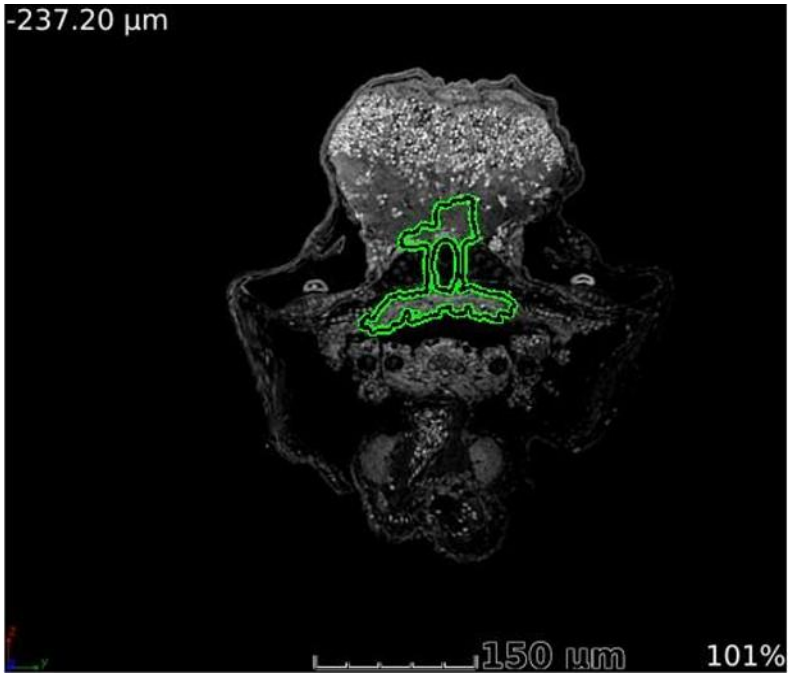

Figure 5-6. Final segmentation using mask 3. Grayscale value = 48.6106

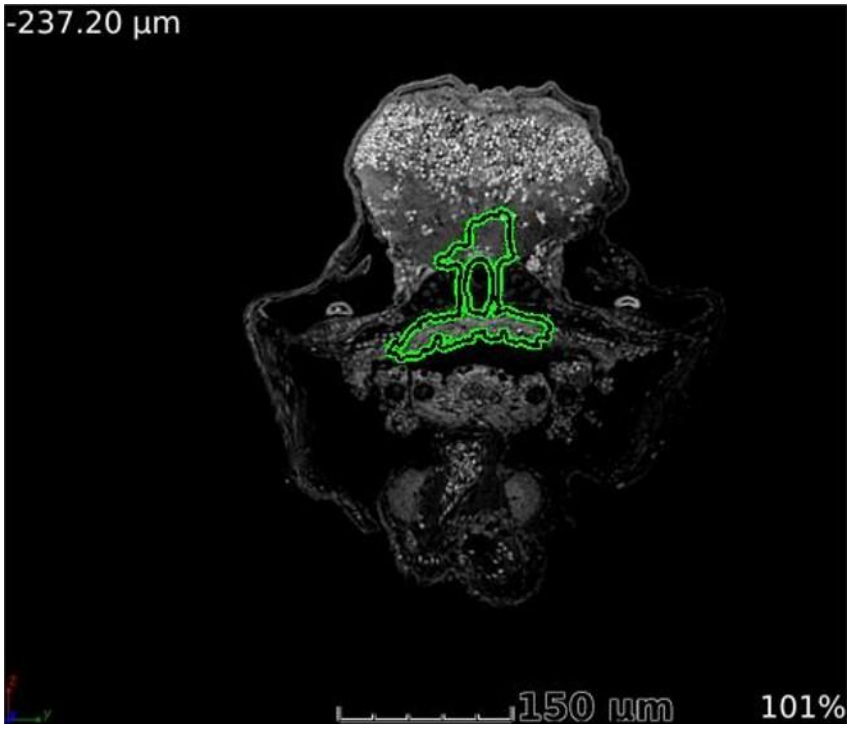

Figure 5-7. Final segmentation using mask 4. Grayscale value = 49.7568

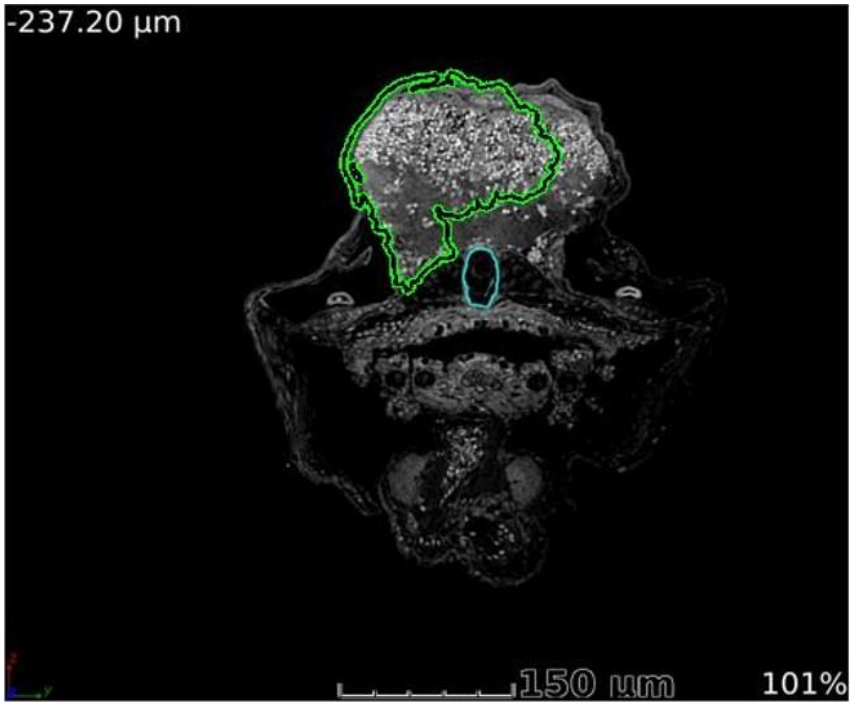

Figure 5-8. Final segmentation using mask 5. Grayscale value = 75.3696

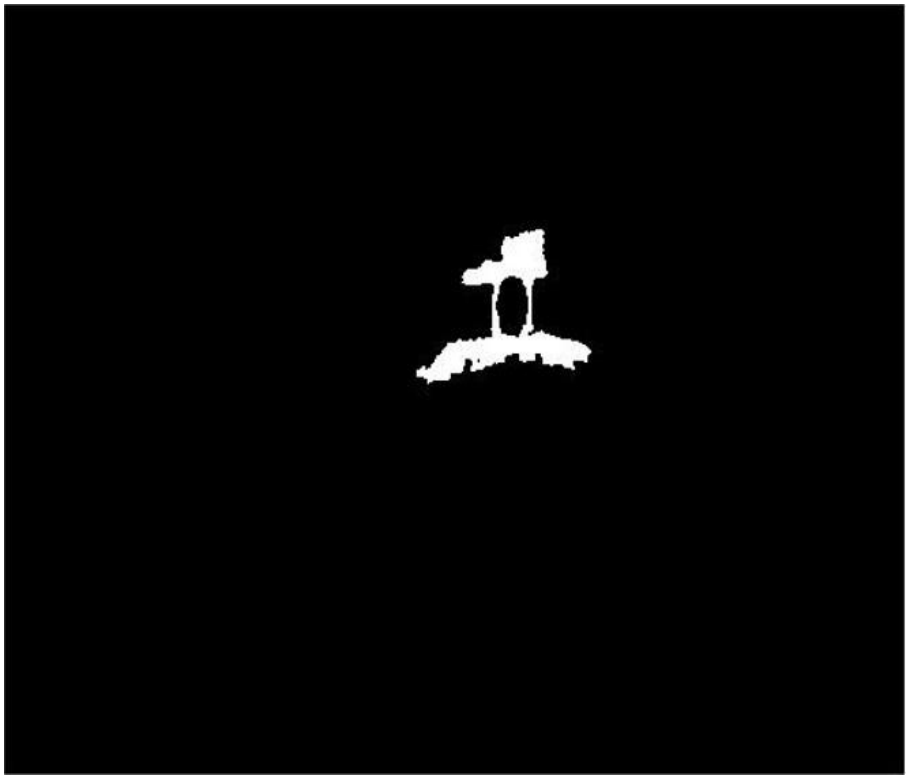

Figure 5-9. Final binary segmented image using mask 3.

From the above images we can see the grayscale value is least for mask 3 and it is selected.

There are several advantages of using the automated approach for selecting the masks. It helps remove human input and thus large sets of images can be segmented quickly. It helps in saving time and also help in research. The next section will explain about the data set being used for this thesis.

Chapter 6

Data Set

The data set consists of CT scan images of Zebrafish obtained by research team at Hershey hospital under Dr. Cheng. The original image obtained is a 3-D image which is around a total of 114 Gigabytes. The 3-D images are processed and a total of 1350 images are provided for my research. The images were processed and labelled with ground-truth images by the research team at Hershey. The objective is to identify and segment out the notochord tissue present in the image of the zebrafish. A sample image of the zebrafish with the notochord has been provided earlier, below I will show a few images which shows the evolution of the notochord tissue through the list of images.

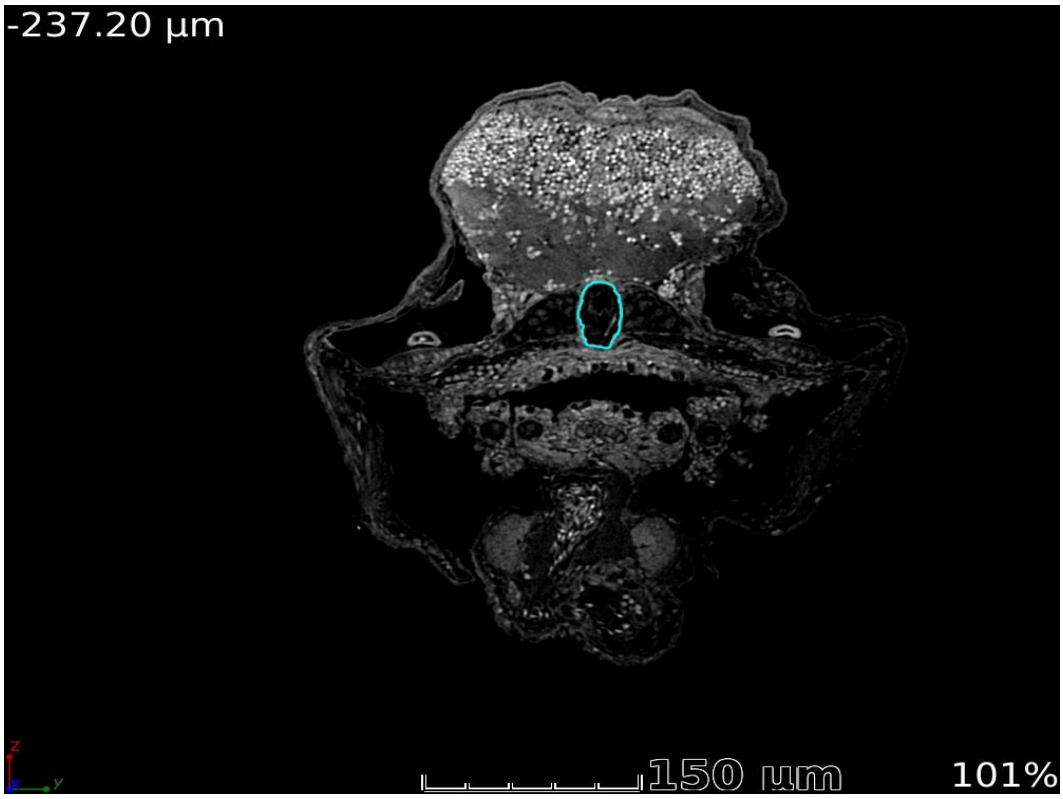

Figure 6-1. Image of the Zebrafish with notochord tissue labelled

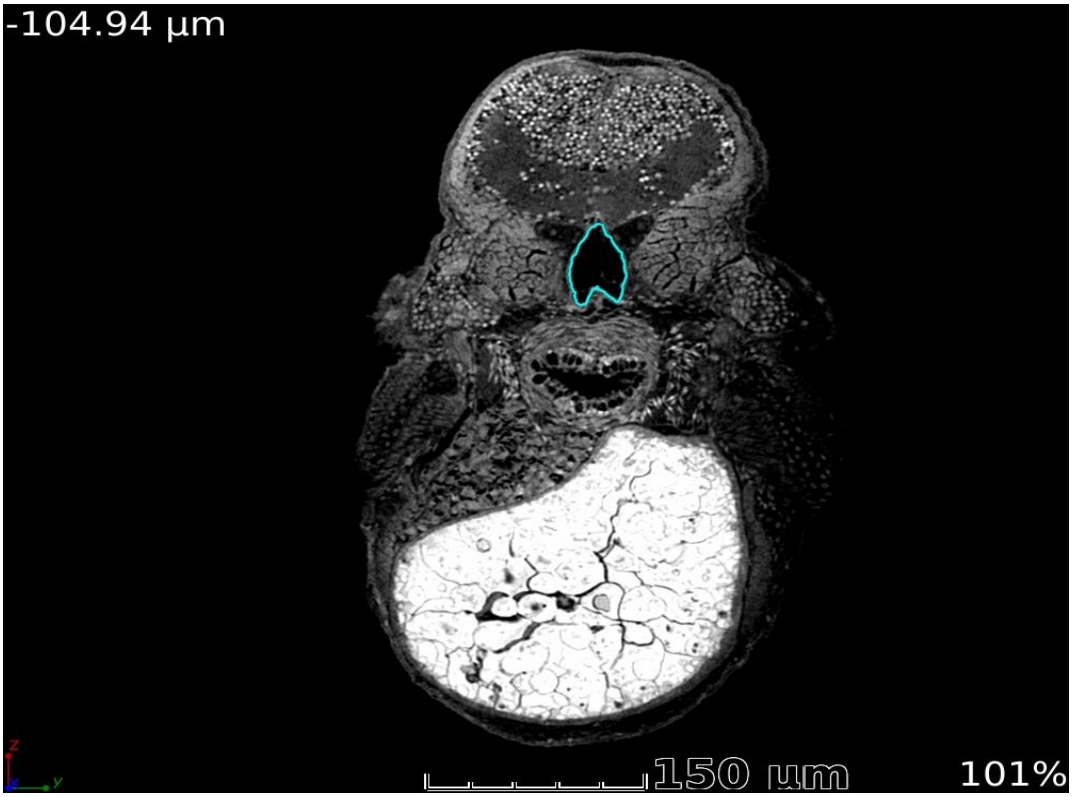

Figure 6-2. Image of the Zebrafish with notochord tissue labelled.

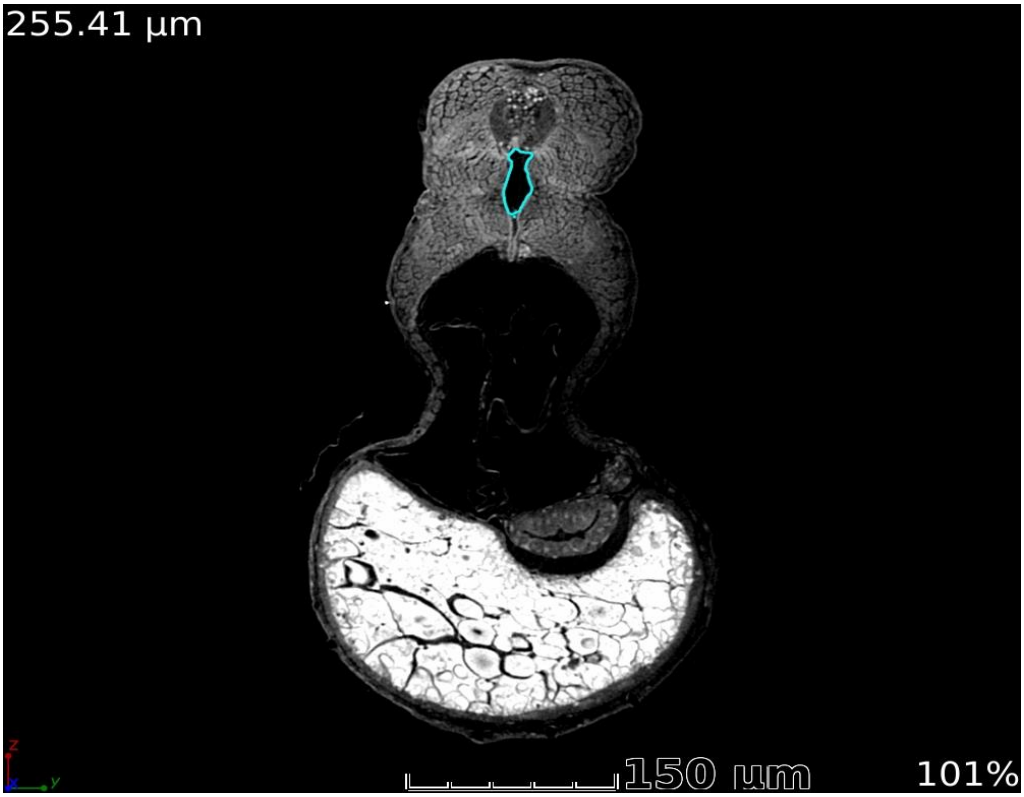

Figure 6-3. Image of the Zebrafish with notochord tissue labelled.

Figure 6-4. Image of the Zebrafish with notochord tissue labelled.

Chapter 7

Experimental Results and Observations

Following experimentation and results were obtained on the images of zebrafish.

1. Method – I is evaluated on 200 images and the accuracy measures have been calculated.
2. Method – II is evaluated on 500 images and the accuracy measures have been calculated.
3. How well the segmentation algorithm performs with variable number of iterations is observed.
4. How well the segmentation algorithm performs by varying the smoothening parameter from 0 – 1 is observed.
5. How well the segmentation algorithm performs by varying the size of the initial binary mask is observed.

The measures used to assess the accuracy of the algorithm are True Positive Rate and ratio of False Positive Count to True Positive Count.

True Positive Rate is also known as sensitivity. It measures the proportion of pixels of notochord tissue that are correctly identified as notochord tissue. It should be as high as possible.

$$True\ Positive\ Rate = \frac{notochord\ tissue\ pixels\ correctly\ classified}{True\ number\ of\ notochord\ tissue\ pixels}$$

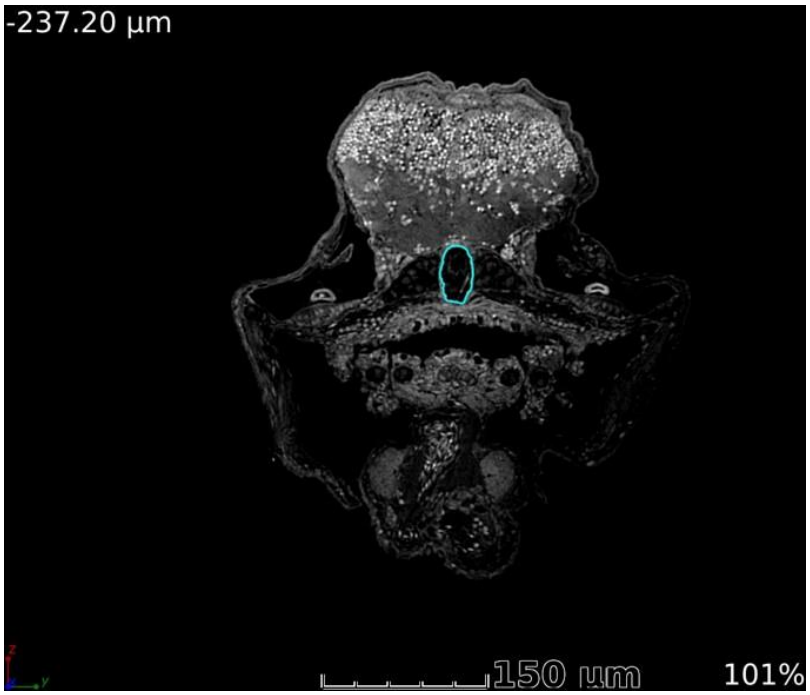

Figure 7-1. Original image with notochord tissue.

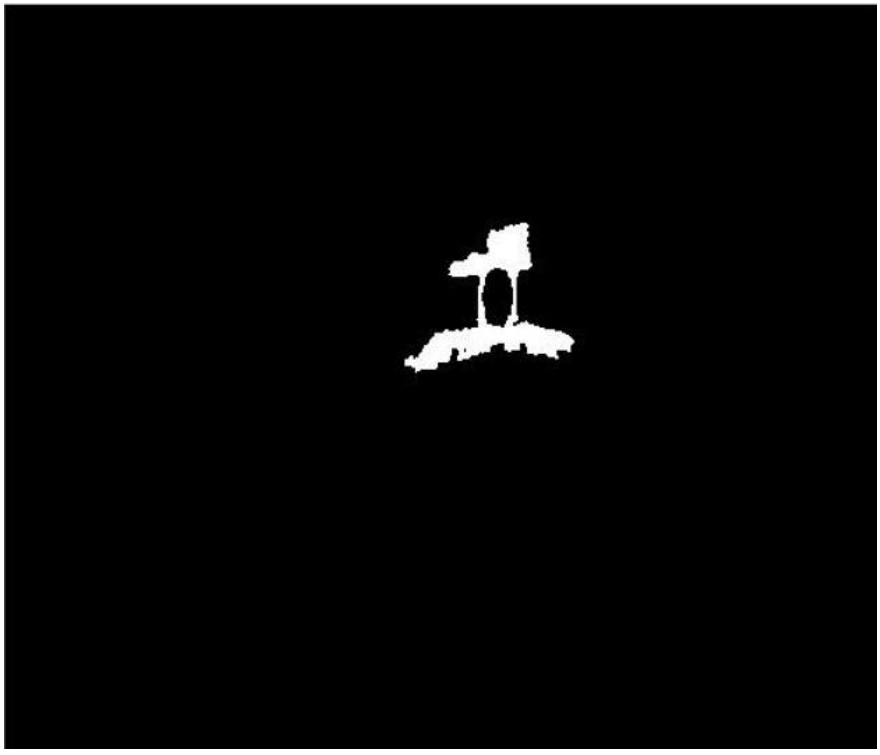

Figure 7-2. Segmented image at the output of the algorithm.

True Positive rate is obtained by comparing the above two images.

Ratio of False Positive Count to True Positive Count. This will help us understand what proportion of the segmented image is incorrectly classified as notochord tissue. This measure was selected as it gives more insight in how successful the segmentation algorithm works. Initially only False Positive rate was chosen, but since this measure takes into account the entire images resulting in a very low rate, it does not necessarily define how well the segmentation has worked. Thus instead of calculating the False Positive rate in a bounding box around the segmented image, the ratio of False Positive count to True Positive count is calculated which will be much more insightful.

$$Proportion\ of\ False\ Positives = \frac{False\ Positive\ Count}{True\ Positive\ Count}$$

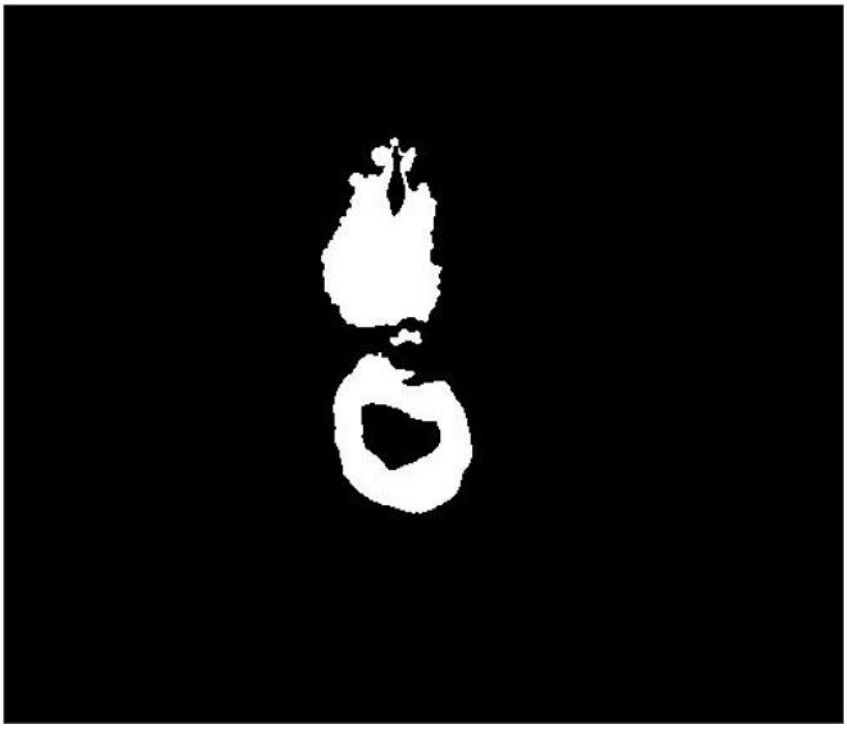

Figure 7-3. Segmented image at the output of the algorithm.

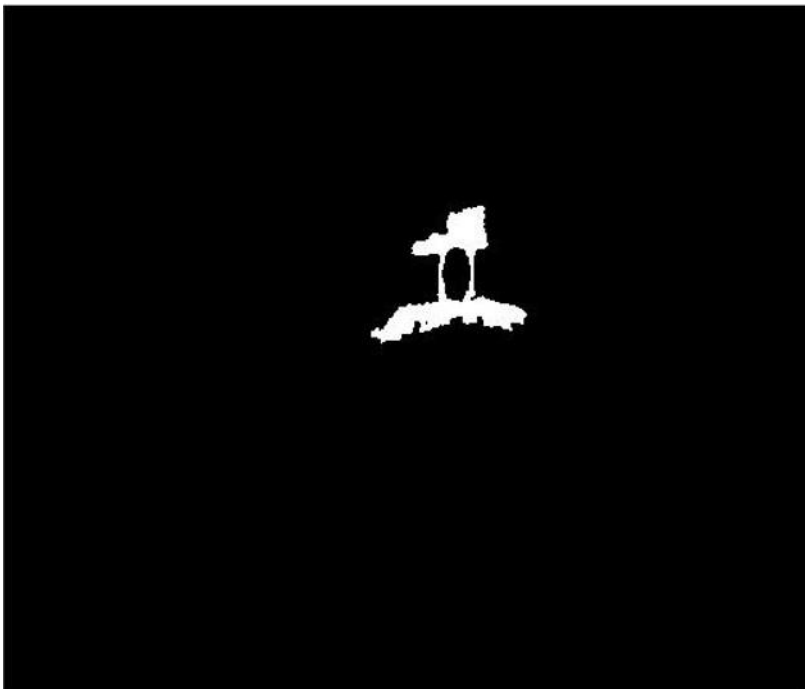

Figure 7-4. Another segmented image at the output of the algorithm.

When we compare images in Figure 7-3. And Figure 7-4. We see that in spite of correctly identifying and segmenting out the notochord tissue for two different images, there is vast difference between the two outputs. The Proportion of False Positives for figure 7-3. will be much higher as compared to the Proportion of False Positives for Figure 7-4. This shows the importance of this particular accuracy measure.

Method – I used for segmentation is where only one binary mask of size 200x110 is used on the images. The mask has been shown previously in Figure 5-1. Method – II is the automated algorithm to select the appropriate mask for each image and then calculate the accuracy measures for the same. The masks used have been shown previously in Figure 5-3. In the following pages the plots for True Positive Rates and ratio of False Positive Count to True Positive Count for the two methods along with observations of the other experiments have been attached.

1. **Results of Method – I which have been evaluated on 200 images are shown below:**

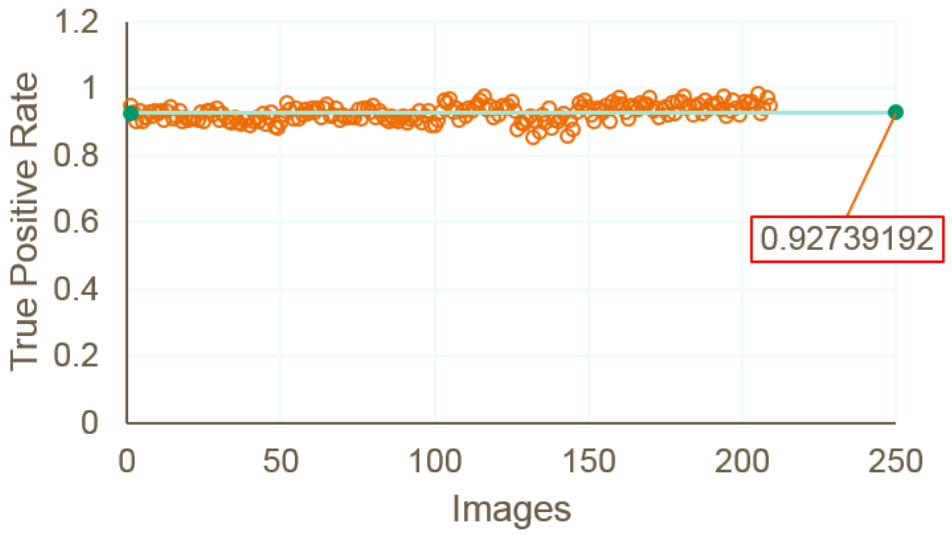

Figure 7-5. True Positive Rates using Method – I on 200 images. Solid orange line indicates the average value.

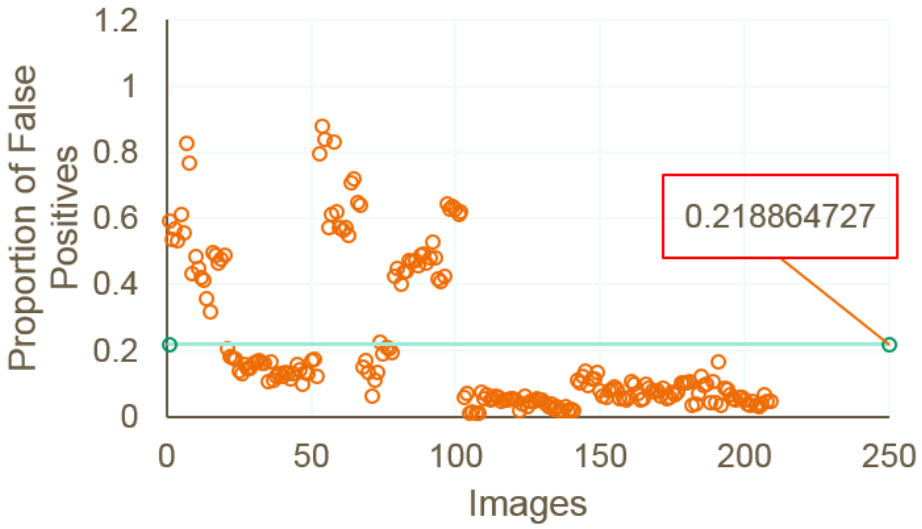

Figure 7-6. Proportion of False Positives using Method – I on 200 images. Solid orange line indicates the average value.

Following observations can be deduced from the approach using a single big mask:

- The 200x110 mask selected is the most appropriate mask for that size to cover all the images with notochord tissue developing.
- Other masks of the same size at different positions have been tried, but they do not help in segmentation for all the images.
- Average True Positive Rate obtained is considerably high and comparable to the previous results obtained.
- Average Proportion of False Positives obtained is slightly on the higher side but acceptable with respect to the True Positive Rate achieved.
- Results are obtained only on 200 images due to very high computation time.

2. **Results of Method – II which have been evaluated on 500 images are shown below:**

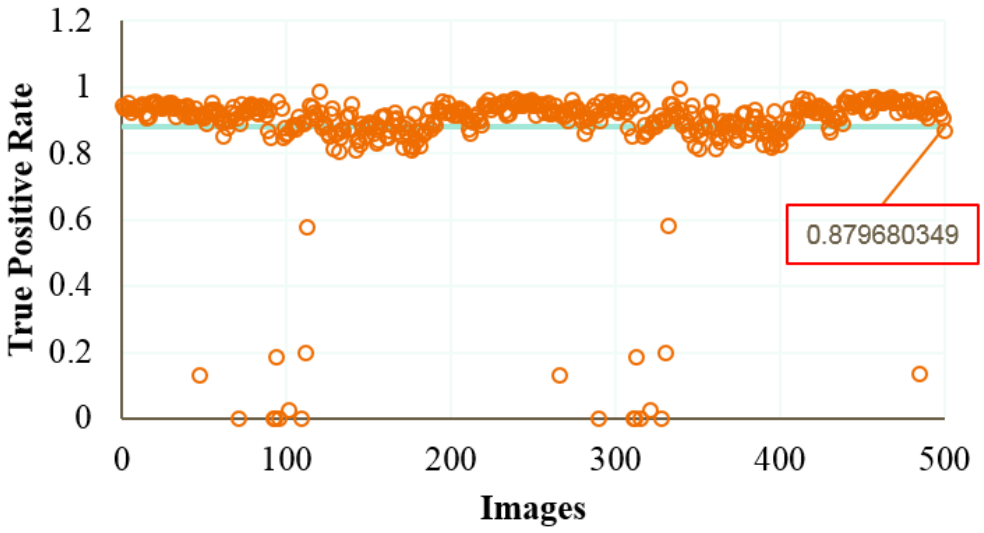

Figure 7-7. True Positive Rate using Method – II on 500 images. Solid orange line indicates the average value.

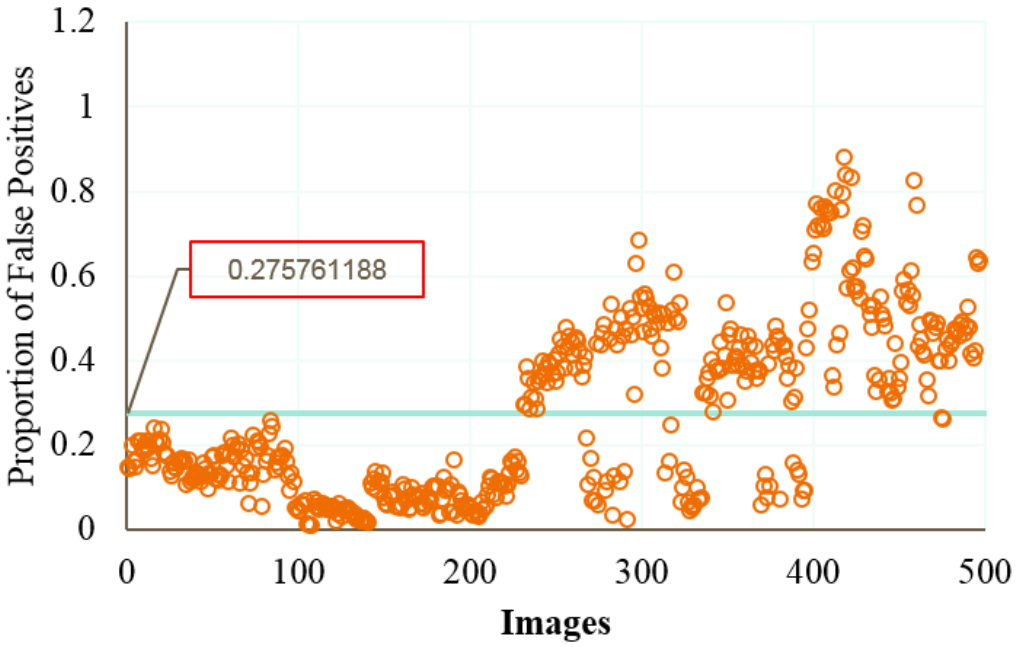

Figure 7-8. Proportion of False Positives using Method – II on 500 images. Solid orange line indicates the average value.

Following observations can be deduced from the automated mask select approach:

- 5 masks of size 20x20 have been randomly selected.
- Segmentation using all the masks on each image is obtained, the best mask for each image is selected based on average grayscale value of the segmented image.
- Average True Positive Rate obtained is lower than the value for the approach using a single big mask, but it is relatively high and an acceptable value.
- Average Proportion of False Positives obtained is lower than the value for the approach using a single big mask which is good.

- The automated algorithm on the whole becomes a very dependable and successful approach to segment out the notochord tissue from the image of zebrafish.
- Number of masks used, can be increased or decreased depending upon ones need.
- The most frequently selected mask amongst the 500 images was mask no 3, followed by mask no 2.
- Least frequently selected mask was mask no 1.

Table 7-1. Frequency of selection of mask for the automated approach.

Mask No	No of times mask is selected
1	**39**
2	**150**
3	**161**
4	**69**
5	**81**

3. **How well the segmentation algorithm performs with variable number of iterations is observed.**

Below are a list of images which show the amount of segmentation obtained with different number of iterations. This change is shown on 2 different images.

Table 7-2. Evolution of contour and segmented image at the end of 100 iterations.

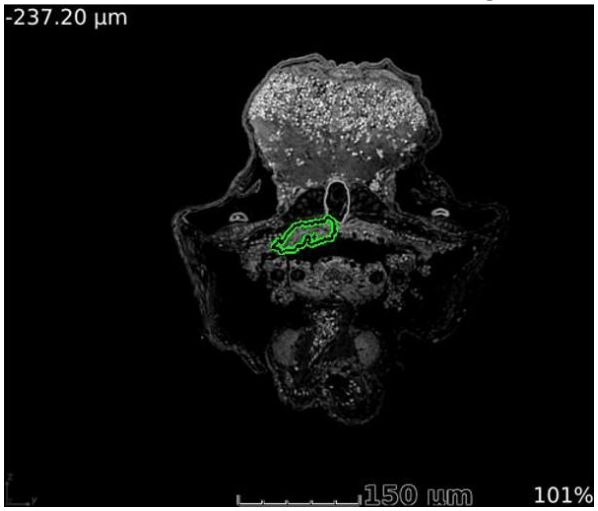

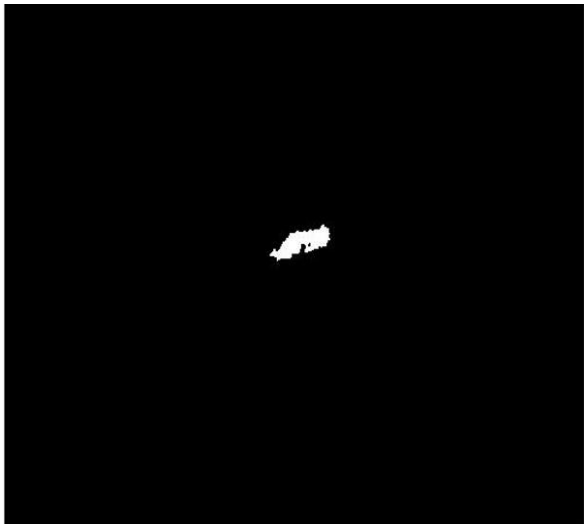

Table 7-3. Evolution of contour and segmented image at the end of 200 iterations.

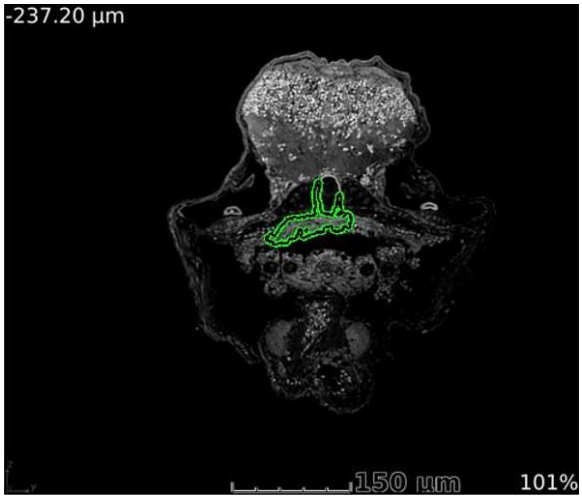

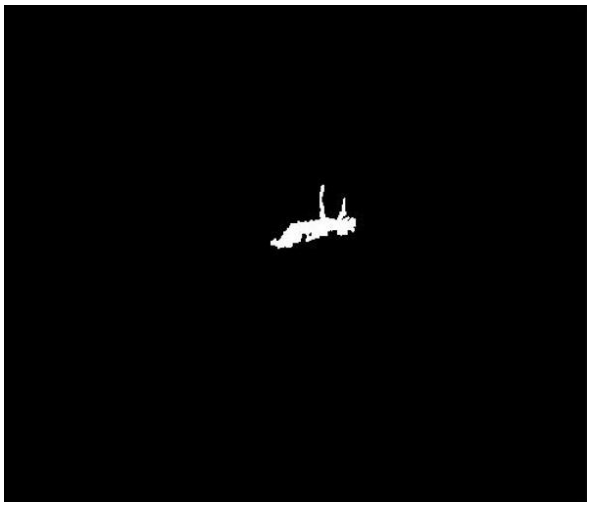

Table 7-4. Evolution of contour and segmented image at the end of 300 iterations.

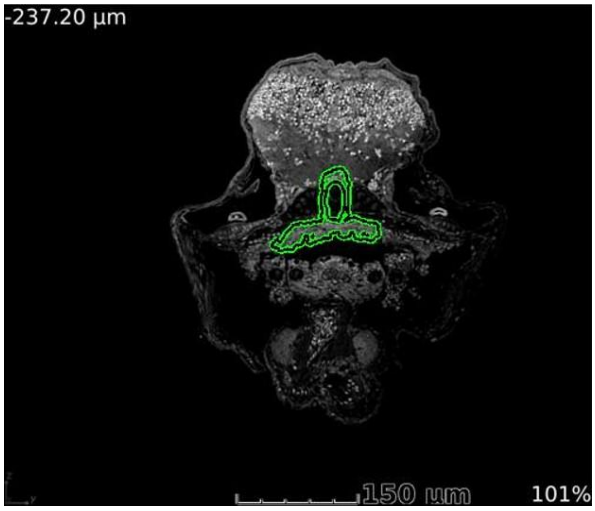

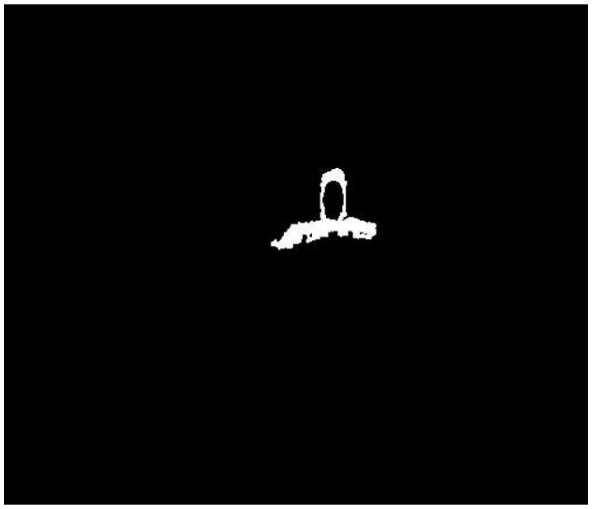

Table 7-5. Evolution of contour and segmented image at the end of 400 iterations.

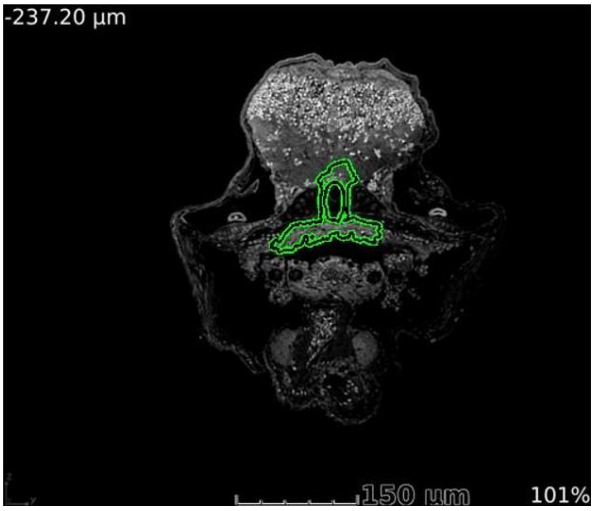

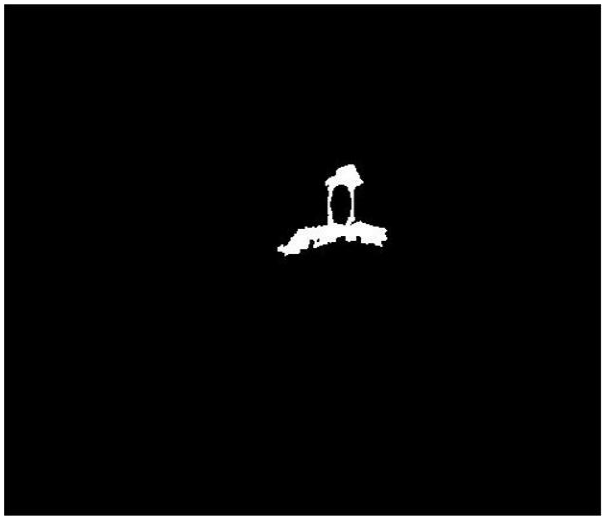

Table 7-6. Evolution of contour and segmented image at the end of 500 iterations.

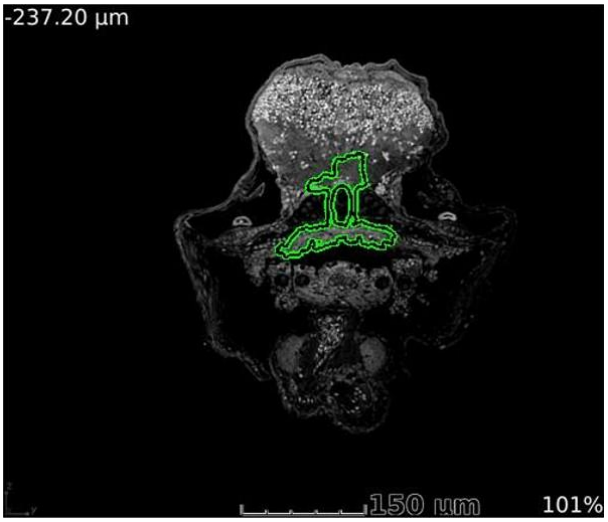

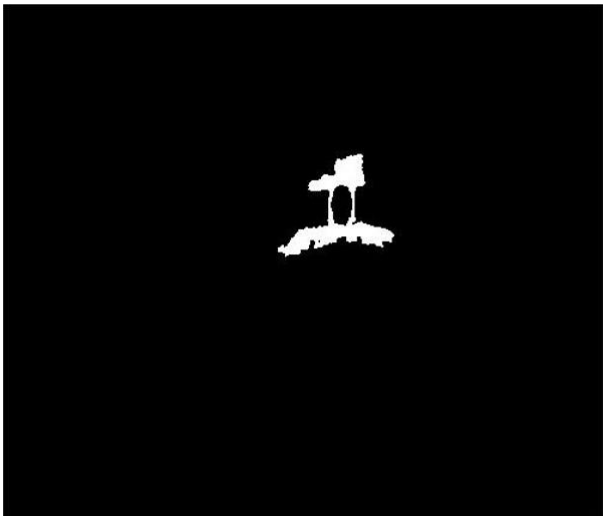

Table 7-7. Evolution of contour and segmented image at the end of 100 iterations.

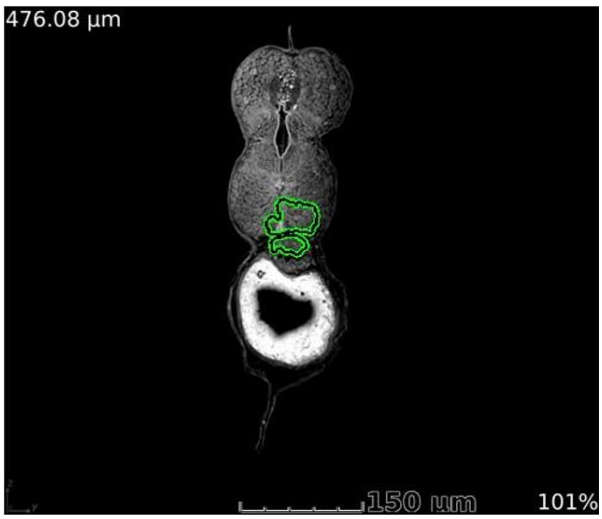

Table 7-8. Evolution of contour and segmented image at the end of 200 iterations.

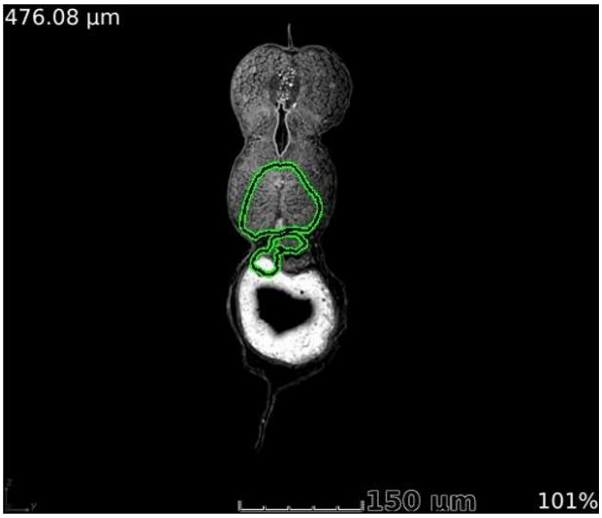

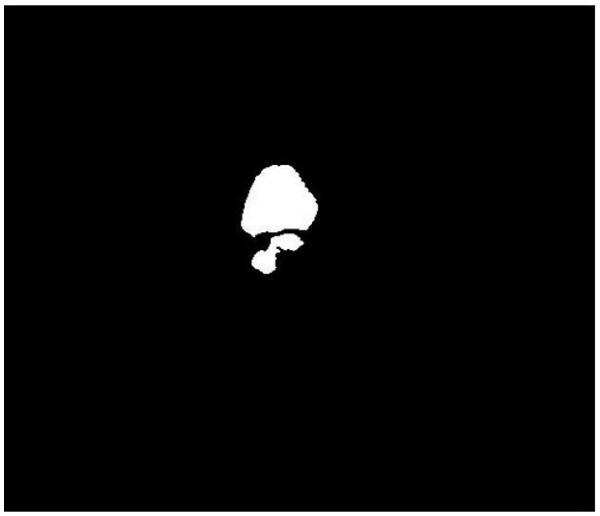

Table 7-9. Evolution of contour and segmented image at the end of 300 iterations.

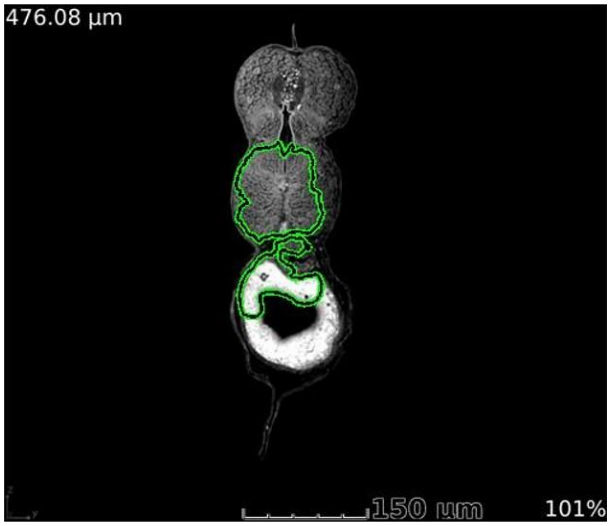

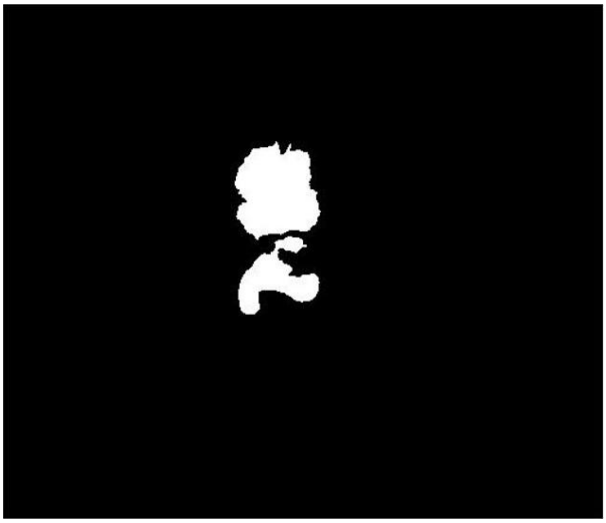

Table 7-10. Evolution of contour and segmented image at the end of 400 iterations.

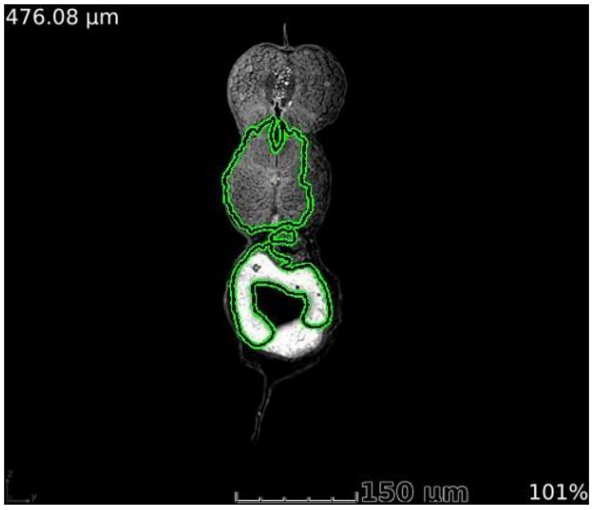

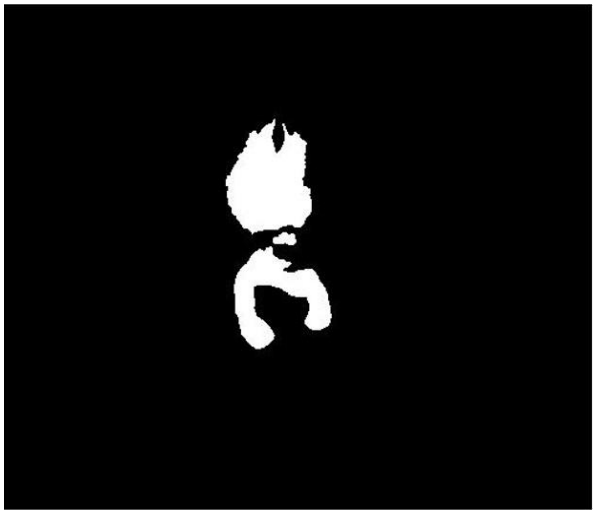

Table 7-11. Evolution of contour and segmented image at the end of 500 iterations.

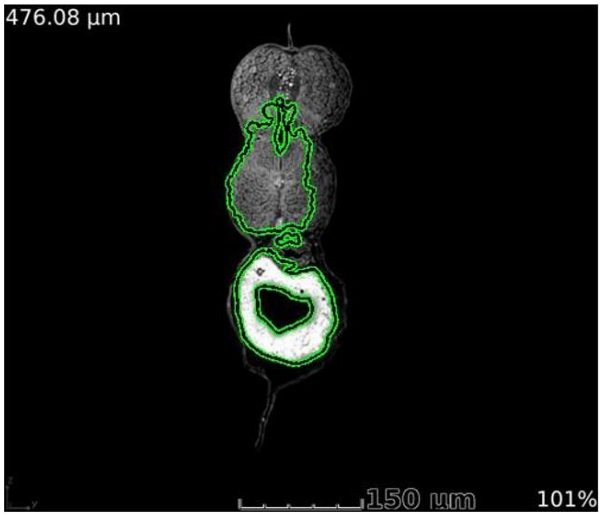

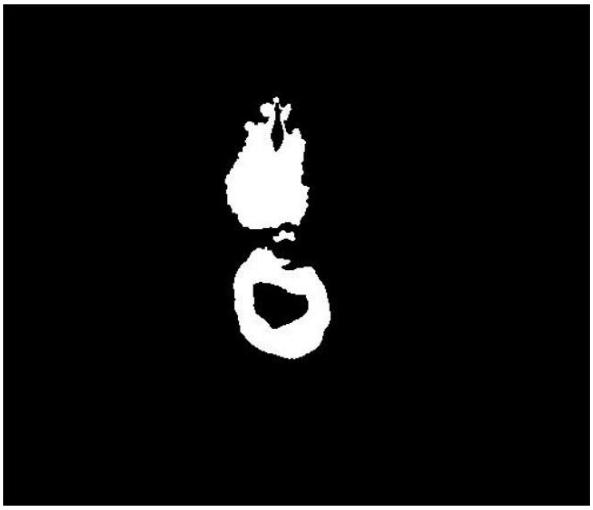

As we can observe from the tables that complete segmentation of the notochord tissue takes place at different number of iterations for different images. For the first image, the ideal number of iterations is 300. Whereas for the second image, the ideal number of iterations is

500. In fact even at the end of 500 iterations the notochord tissue is just segmented completely. Thus there is scope for improvement and future work here. One can modify the algorithm such that, the segmentation process terminates as soon as the complete notochord tissue is segmented out for each image. This will improve the efficiency and the time complexity of the algorithm also.

4. **How well the segmentation algorithm performs by varying the smoothening parameter from 0 – 1 is observed.**

The smoothening parameter helps in making the curve smoother. Its value ranges from 0 to 1. This value is added to the curve, after minimizing the energy term using narrow band level sets. We have taken the default value of this parameter to be 0.2 in this thesis. This value had been chosen experimentally after varying it and measuring the accuracy on 200 random images. The table below will show changes brought about by changing the value of this parameter.

Table 7-12. Performance measure by varying the smoothening parameter.

Value of Smoothening Parameter	True Positive Rate	Proportion of False Positives
0.1	**0.84932**	**0.250359**
0.2	**0.872724**	**0.300501**
0.3	**0.862107**	**0.291888**
0.4	**0.866205**	**0.273662**
0.5	**0.868943**	**0.316934**
0.6	**0.868608**	**0.328123**
0.7	**0.823733**	**0.327975**
0.8	**0.783171**	**0.347112**
0.9	**0.747436**	**0.409198**
1	**0.714928**	**0.437761**

From the above table we can see that, as the smoothening parameter increases the accuracies decrease and the segmentation becomes worse. We can choose the smoothening parameter to be any of the initial values. I have chosen 0.2 to be the default value but this will change for a different data set of images where the object of interest is different.

5. **How well the segmentation algorithm performs by varying the size of the initial binary mask is observed.**

Experimentation is performed with 4 different sizes of the mask. The masks are strategically kept in the top left corner, as we have prior knowledge on how the notochord tissue develops. The four masks are then evaluated on 200 random images and their performance measure is measured. Below are the representations of the 4 masks with one particular image from the data set.

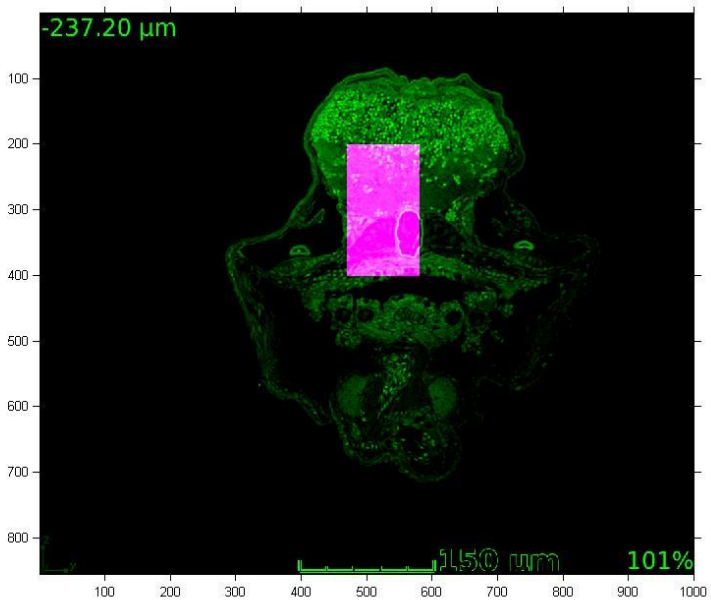

Figure 7-9. Mask of same size as input image. Rectangular patch of 1's defined as mask1 (200:400,470:580) = 1.

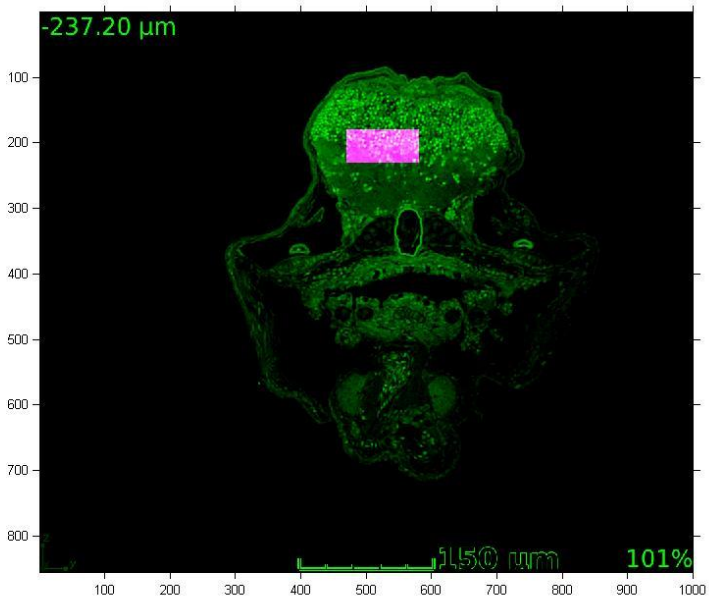

Figure 7-10. Mask of same size as input image. Rectangular patch of 1's defined as mask2 (180:230,470:580) = 1.

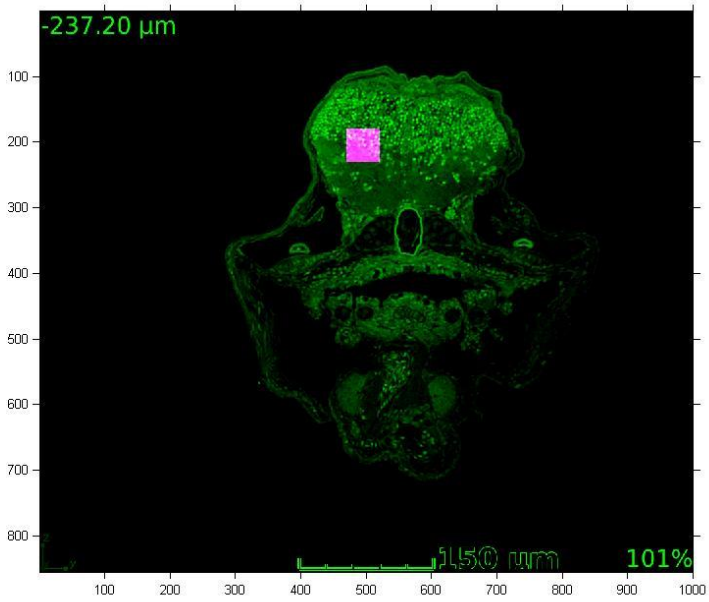

Figure 7-11. Mask of same size as input image. Rectangular patch of 1's defined as mask3 (180:230,470:520) = 1.

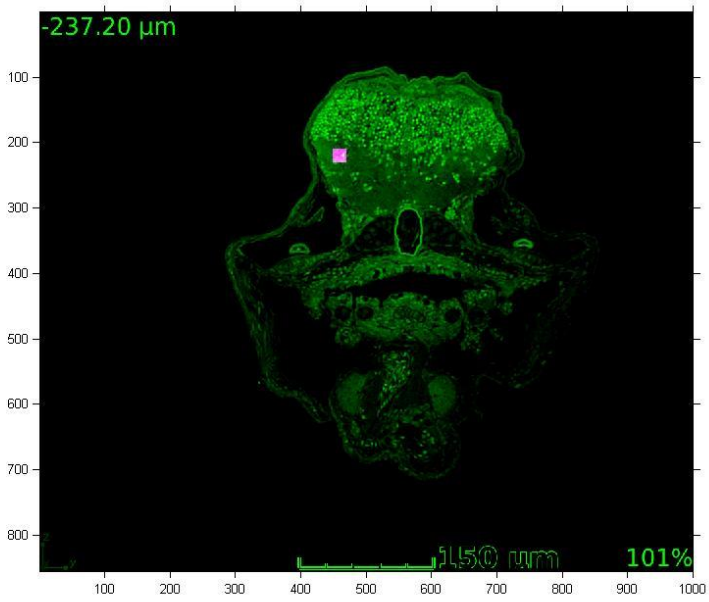

Figure 7-12. Mask of same size as input image. Rectangular patch of 1's defined as mask4 (210:230,450:470) = 1.

The table below will show the performance of these masks on 200 random images:

Table 7-13. Performance of masks of different sizes.

Mask No	True Positive Rate	Proportion of False Positives
mask1	**0.808397**	**0.354966**
mask2	**0.788585**	**0.409198**
mask3	**0.826979**	**0.345813**
mask4	**-**	**-**

From the above table we can observe that as the size of the mask reduces, we can achieve better accuracies. Values for mask4 are not present because the program threw an error. This is because since the patch of 1's is of a very small size of 20 x 20, only one small mask will not work for all the images. In order to use a mask of such small size, we will have to use Method – II and define multiple masks, such that there may or may not be a unique mask for each image. By using a smaller mask, the redundancies will reduce and also the computations will be much faster. Thus I suggest that one must use Method – II and define multiple small masks.

Chapter 8

Conclusion and Future Work

At the end of this thesis I would like to conclude by saying that the desired level of segmentation accuracy has been achieved. Unsupervised method to identify and segment the notochord tissue works well. The automated approach that has been suggested, can be deployed by the researchers at Hershey with slight modifications almost immediately. The algorithm will help move forward the research, and at the same time provide great results. The automated algorithm proposed provides better efficiency and also has not been proposed earlier in literature. This algorithm is weakly supervised and can be used for other segmentation problems in other domains of biomedical engineering and medicine. It can help in research and help cure many problems in the field of medicine. I can proudly suggest that I have done justice to this research up to my best abilities with great help from Dr. Miller in the given time span. He has provided me with great guidance throughout my thesis and has advised me very well over the past year.

Having said all this about this particular research area and to be specific this topic, it still has potential for further improvement. True Positive Rates can be increased further, while the Proportion of False Positives can be reduced further with modifications. The hyper-parameters such as number of iterations, appropriate value of smoothening parameter, size of the mask should be selected more precisely with more experimentation. It will differ for different data sets. The number of iterations can be reduced further and the algorithm could be designed to stop the segmentation as soon as the notochord tissue has been segmented out successfully. As mentioned earlier, this will improve the efficiency and the time complexity. This could be a very interesting research topic for a potential PhD candidate. I would like to wish luck to whosoever continues this research. I would like to conclude by thanking Pennsylvania State University, Dr. Miller and Dr. Doherty for this amazing opportunity. It has been a wonderful journey.

References

1. Chan, Tony F., and Luminita A. Vese. "Active contours without edges." *Image processing, IEEE transactions on 10,* no. 2 (2001): 266-277.

2. Kass, Michael, Andrew Witkin, and Demetri Terzopoulos. "Snakes: Active contour models." *International journal of computer vision 1,* no. 4 (1988): 321-331.

3. Kichenassamy, Satyanad, Arun Kumar, Peter Olver, Allen Tannenbaum, and Anthony Yezzi. "Gradient flows and geometric active contour models." *In Computer Vision, 1995. Proceedings, Fifth International Conference on,* pp. 810-815. IEEE, 1995.

4. Lankton, Shawn. "*Sparse field methods-technical report.*" Georgia institute of technology (2009).

5. Mumford, David, and Jayant Shah. "Optimal approximations by piecewise smooth functions and associated variational problems." *Communications on pure and applied mathematics 42,* no. 5 (1989): 577-685.

6. Osher, Stanley, and Ronald P. Fedkiw. "Level set methods: an overview and some recent results." *Journal of Computational physics 169,* no. 2 (2001): 463-502.

7. Osher, Stanley, and James A. Sethian. "Fronts propagating with curvature-dependent speed: algorithms based on Hamilton-Jacobi formulations." *Journal of computational physics 79,* no. 1 (1988): 12-49.

8. Tsai, Richard, and Stanley Osher. "Review article: Level set methods and their applications in image science." *Communications in Mathematical Sciences 1,* no. 4 (2003): 1-20.

9. Whitaker, Ross T. "A level-set approach to 3D reconstruction from range data." *International journal of computer vision 29,* no. 3 (1998): 203-231.

10. Xu, Chenyang, and Jerry L. Prince. "Snakes, shapes, and gradient vector flow." *Image Processing, IEEE Transactions on 7,* no. 3 (1998): 359-369.

11. Zhu, Song Chun, and Alan Yuille. "Region competition: Unifying snakes, region growing, and Bayes/MDL for multiband image segmentation." *Pattern Analysis and Machine Intelligence, IEEE Transactions on 18,* no. 9 (1996): 884-900.

12. *https://math.berkeley.edu/~sethian/2006/Explanations/level_set_explain.html*

13. *http://www.mathworks.com/matlabcentral/fileexchange/19567-active-contour-segmentation*